## General Disclaimer

## One or more of the Following Statements may affect this Document

- This document has been reproduced from the best copy furnished by the organizational source. It is being released in the interest of making available as much information as possible.

- This document may contain data, which exceeds the sheet parameters. It was furnished in this condition by the organizational source and is the best copy available.

- This document may contain tone-on-tone or color graphs, charts and/or pictures, which have been reproduced in black and white.

- This document is paginated as submitted by the original source.

- Portions of this document are not fully legible due to the historical nature of some of the material. However, it is the best reproduction available from the original submission.

NASA CONTRACTOR
REPORT

NASA CR-61268

March 20, 1969

NASA CR-61268

# SLOSH TEST ANALYSIS FOR THE 200-INCH MULTICELL TANK

Prepared under Contract No. NAS 8-20073 by
J. C. Walls and C. E. McCandless

BROWN ENGINEERING COMPANY, INC.



For

NASA-GEORGE C. MARSHALL SPACE FLIGHT CENTER
Marshall Space Flight Center, Alabama

March 20, 1969

NASA CR-61268

# SLOSH TEST ANALYSIS FOR THE 200-INCH MULTICELL TANK

By

J. C. Walls and C. E. McCandless

Prepared under Contract No. NAS 8-20073 by

BROWN ENGINEERING COMPANY, INC.

For

Astronautics Laboratory



NASA-GEORGE C. MARSHALL SPACE FLIGHT CENTER

# SLOSH TEST ANALYSIS FOR THE 200-INCH MULTICELL TANK

By

J. C. Walls
C. E. McCandless

ABSTRACT

Analytical expressions for liquid natural frequencies, forces, moments, pressures, and surface displacement are determined for a ten-sector circular compartmented tank, geometrically equivalent to the 200-inch multicell tank. Slosh test results for the 200-inch multicell tanks are then compared to these analytically determined values. In general, excellent correlation is obtained for natural frequencies, forces, moments, pressure, and surface displacements of the liquid, considering the complexity and nonlinearities of the problem.

TABLE OF CONTENTS

## LIST OF ILLUSTRATIONS

LIST OF ILLUSTRATIONS (Concluded)



LIST OF TABLES

## DEFINITION OF SYMBOLS

$a$ = outer tank radius

$b$ = inner tank radius

$d$ = diameter

$F$ = force

$g$ = gravitational acceleration

$h$ = liquid depth

$i = \sqrt{-1}$

$J_\nu$ ( ) = Bessel function of first kind of order $\nu$

$M$ = moment

$M_f$ = total mass of liquid

$p$ = normal pressure

$r$ = radial coordinate

$t$ = time

$x,y,z$ = rectangular coordinate axes

$\alpha$ = vertex angle of sector tank

$\bar{\alpha} = 2\pi\alpha$

$\Gamma$ = gamma function

$\delta$ = displacement of liquid free surface from equilibrium position with respect to space coordinate

$\zeta = \epsilon_{mn} \frac{z}{a}$

$\eta = \Omega_i/\omega_{mn}$

$\phi$ = angular coordinate

$\kappa = \epsilon_{mn} h/a$

$\rho$ = liquid mass density

## DEFINITION OF SYMBOLS (Concluded)

$\sigma = \epsilon_{mr}\, r/a$

$\Phi$ = velocity potential function

$\Omega$ = excitation frequency

$\omega$ = natural circular frequency

$f = \omega/2\pi$

$m,n,\mu$ = series indices

$x_o, y_o$ = amplitude of forcing excitation in x and y directions.

## UNUSUAL TERMS

Sloshing: All stable oscillatory liquid motion.

Splashing: All unstable oscillatory liquid motion.

## CONVERSION TO METRIC SYSTEM

To convert inches to meters, multiply by $2.54 \times 10^{-2}$

To convert pounds mass(avoir.) to kilograms, multiply by $4.5359 \times 10^{-1}$

To convert psi to Newtons per square meter, multiply by $6.8948 \times 10^{3}$

# SLOSH TEST ANALYSIS FOR THE 200-INCH MULTICELL TANK


## SUMMARY

A ten-sector, circular, cylindrical compartmented tank, geometrically equivalent to the 200-inch Multicell Tank, is investigated. Analytical expressions are determined for liquid natural frequency, pressure, surface displacement, forces, and moments for this equivalent tank with lateral excitations identical to those in the test tank. First and second analytical liquid natural frequencies are determined which agree very closely with those obtained from the multicell test. Data on forces, moments, and pressures generated by lateral excitation of the test tank are in good agreement with analytically expected values, considering the nonlinearities involved. Liquid surface displacement determined analytically agrees very well with the wave shape observed experimentally.

It is concluded that analytical expressions for liquid natural frequency, forces, moments, etc., obtained by using an equivalent circular compartmented tank are adequate to predict the behavior of liquid in a multicell tank.

It is also concluded that the multicell tank provides efficient means of reducing sloshing masses and increasing liquid resonant frequencies over those of a circular cylindrical tank.


## SECTION I. INTRODUCTION

### A. General Background

Launch vehicles of importance in space technology have liquid fuel which comprises an enormous percentage of their initial weight. Consequently, the dynamic forces resulting from translational, yaw, pitching, and roll motions of these large liquid masses could be very substantial, even beyond the capabilities of the control system to counteract them or the structure to resist them. The control system natural frequencies, the elastic body frequencies, and the fuel-slosh frequencies should all be fairly widely separated due to the possibility of coupling between various components. If the dominant fuel-slosh frequencies are close to any of the control system frequencies, an instability in the flight characteristics can result; and if the fuel-slosh frequencies are close to the elastic body bending frequencies, a large amplitude dynamic response problem may arise.

Control of the liquid dynamic behavior is generally accomplished either by the introduction of various arrangements of baffles (intended to provide an adequate degree of damping in the liquid system) or by modifying the tank geometry in such a way as to change drastically the liquid frequencies.

It should be noted that both the liquid-slosh frequencies and the elastic-body bending frequencies decrease with increasing tank diameter. Since compartmentation, or subdivision, of the tank has a very marked effect on increasing the propellant slosh frequencies it would appear to be an ideal method of avoiding coupling with the rigid body motions. However, the question of relative advantages of the circular-versus-compartmented-tank-configuration is quite complex. Consideration must be given to several factors including weight and fabrication expense. However, as diameters increase for advanced vehicles beyond Saturn V, compartmention may be necessary.

The multicell tank is one of the most promising solutions to this problem, as it offers the following advantages with respect to liquid sloshing:

1. Principal structural elements serve as damping baffles.
2. The shear webs reduce circular sloshing substantially.
3. The masses of the sloshing liquid are decreased considerably.
4. Higher resonant frequencies result.

These advantages were to be verified by tests of the 200-Inch Multicell Tank.

The slosh test of the 200-Inch Multicell Tank was conducted by Brown Engineering Company during February, 1968 at the Marshall Space Flight Center Propulsion and Vehicle Engineering Laboratory Structural Test Facilities. The test was performed according to the test procedures described in Reference (1) and the test results are documented in Reference (2). The test program was monitored by the Structures Division of R-P&VE.

## B. Objectives

The primary objective of the slosh test on the 200-Inch Multicell Tank was to determine the first mode resonant slosh frequency at the 1/2- and 3/4- full levels. Secondary objectives were to determine pressures at various points in the tank, sloshing forces and moments generated, liquid surface displacements, and stresses and strains produced in the webs and cylindrical sections. (See Reference 2.)

The objectives of this report are to calculate natural frequencies, forces, moments, surface displacements, pressures, etc., for a tank geometrically equivalent to the 200-Inch Multicell tank, and to compare the test results with these analytical values.

## SECTION II. TEST SPECIMEN

The test specimen which is the subject of this analysis is a 1/3 scale model of the NOVA segmented tank. The diameter of the model is 508 cm (200 inches). The specimen is referred to in this paper by its common nomenclature, the "Multicell Tank." See Figure 1. (Skirt not shown.)

The configuration of the Multicell Tank, termed "scolloped," somewhat resembles a cluster of tanks; structurally, however, the Multicell Tank differs completely from a tank cluster.

The Multicell Tank is constructed of ten symmetrical segments having common stiffened bulkheads which carry load but, being perforated, do not isolate the liquid content of one segment from another. These bulkheads serve as slosh baffles. The Z-bar stiffeners are arranged vertically on one side of a bulkhead, and horizontally on the other side of the same bulkhead; these stiffeners damp fluid motion in their immediate vicinity.

The mid-section of each segment is a cylindrical surface whose axis is oriented in the flight direction. Immediately joining the cylindrical segment at both its forward (top) and aft (bottom) ends are spherical segments. A radial conical segment joins each spherical segment, forming the forward and aft bulkhead segments. An axial center tube joins all ten segments.

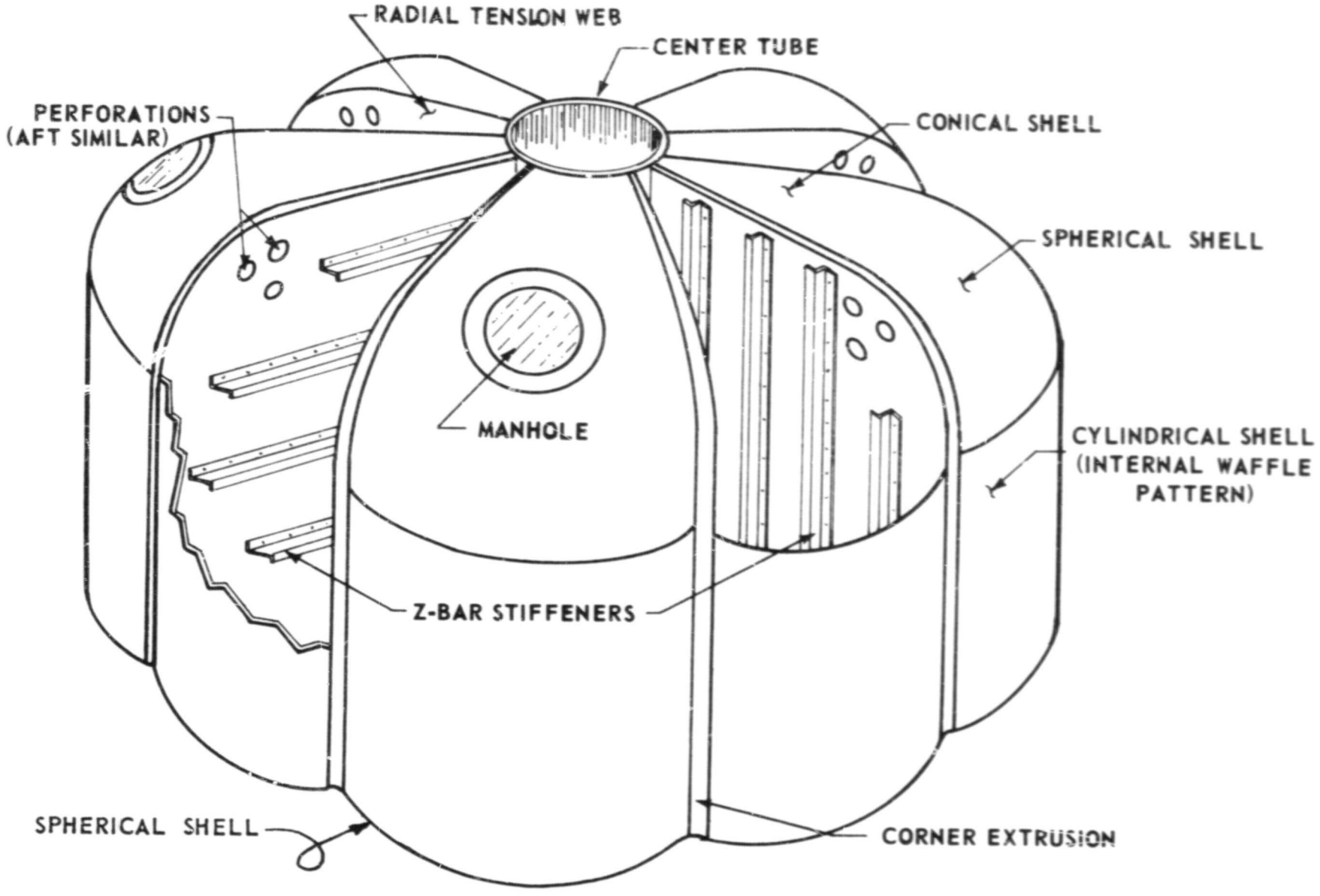


FIGURE 1. MULTICELL TANK

## SECTION III. TEST DATA

### A. Data Required

The primary data requirements for the slosh tests were (1) to determine the first resonant slosh frequency (2) to determine corresponding pressures and strains on the webs and on the cylindrical sections of the tank (3) to obtain horizontal shaker loads (4) to obtain horizontal shaker displacements and (5) to obtain vertical load changes on the ten load feet.

### B. Instrumentation

Cell webs were instrumented with biaxial strain gages, uniaxial strain gages, and pressure transducers.

Outer walls of the cells were instrumented with biaxial strain gages, pressure transducers, and slosh sensors.

Selected cells had slosh sensors located on an inner wall (or in one cell corner) to take advantage of the particular direction of slosh motion.

Each of the ten load feet was equipped with two biaxial strain gages.

Instrumentation location is shown in Figure 2.

### C. Equipment

The following equipment was assembled for the test setup:

A base frame with ten fixed mounting pads equipped with an oil pressurization system; a loading ring with ten integral load feet, each separated from a mounting pad by an oil film, and each instrumented to serve as a load cell; a hydraulic pump; a hydraulic power unit and distributor; a hydraulic shaker and load cell; roller guides and frame to prevent motion at right angles to the shaker displacement; a two-foot displacement transducer; a water-level gage; three TV cameras equipped with zoom lens; two recorders; five oscillographs; and three movie cameras (interchanged with TV cameras during the test).

The base frame and loading ring were carefully leveled, and the axis of the hydraulic shaker was aligned exactly on the diameter of the tank.

### D. Methodology

1. Fluid Level. Since sloshing in a nearly full or a nearly empty tank is of small consequence, two fluid (water) levels were selected for this test: the 1/2-full level and the 3/4-full level.

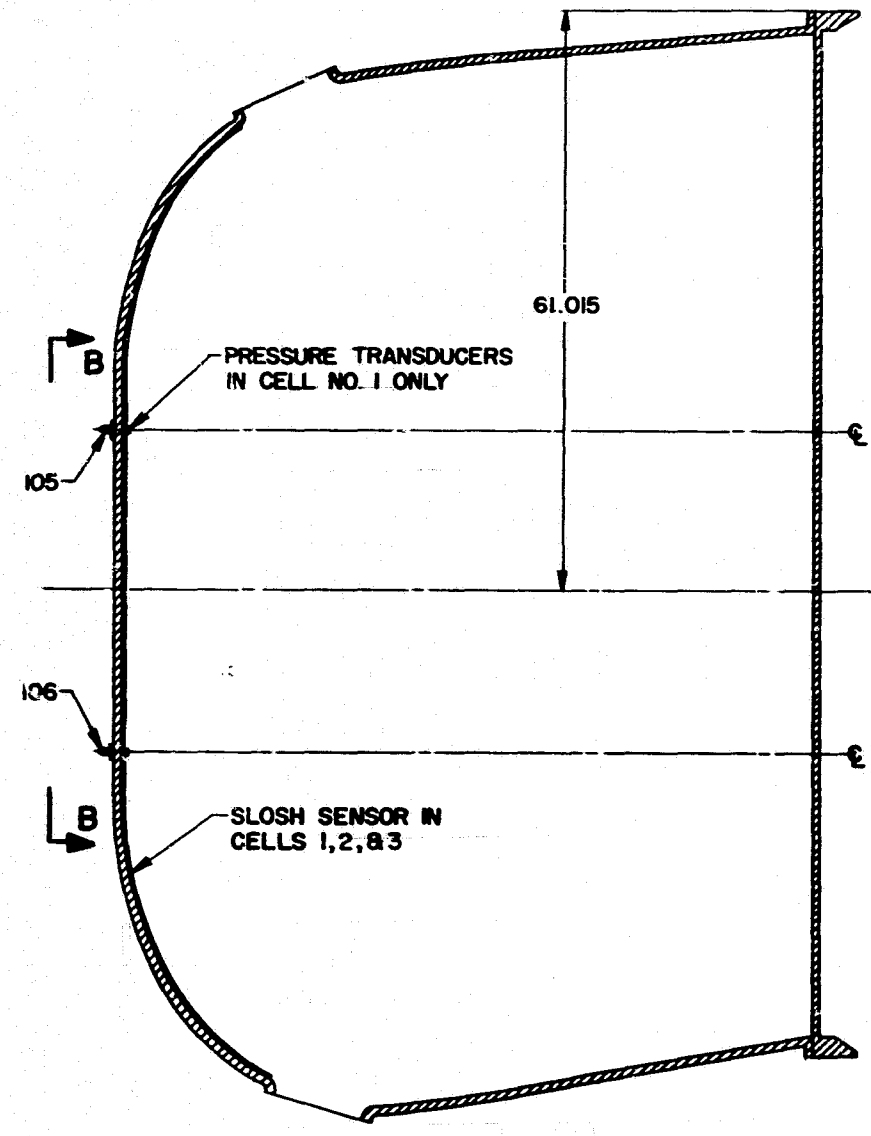


SECTION – AA

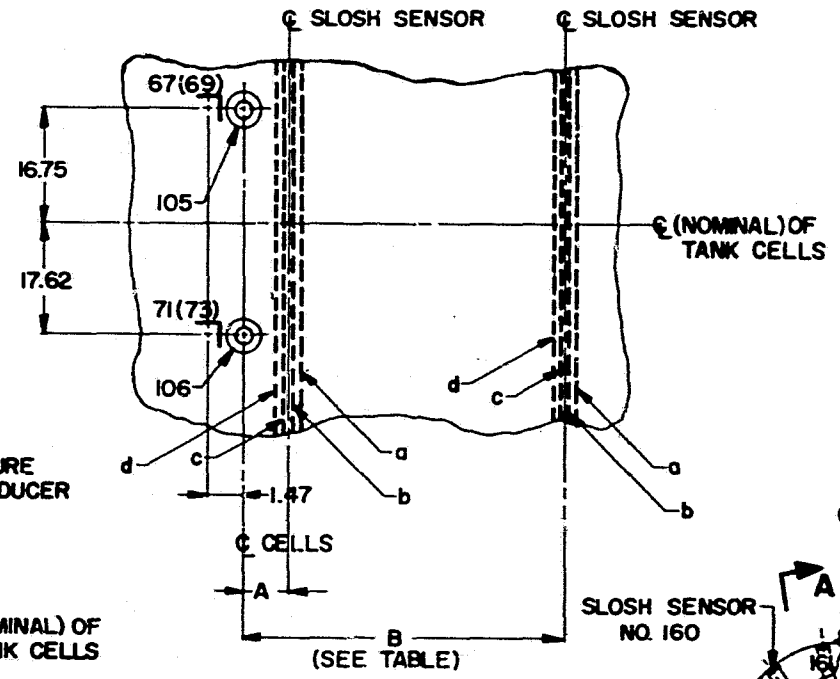


VIEW – BB
(STRAIN GAGES FOR CELL NO. 1 ONLY)

| DIMENSIONS ARE FROM ℄ OF CELL | | |
|---|---|---|
| CELL NO. | DIM. A | DIM. B |
| 1 | .94 | 10.93 |
| 2 | 22.38 | 31.69 |
| 3 | NONE | 31.69 |

NOTE:
NUMBERS 1 THRU 10 IDENTIFY CELLS

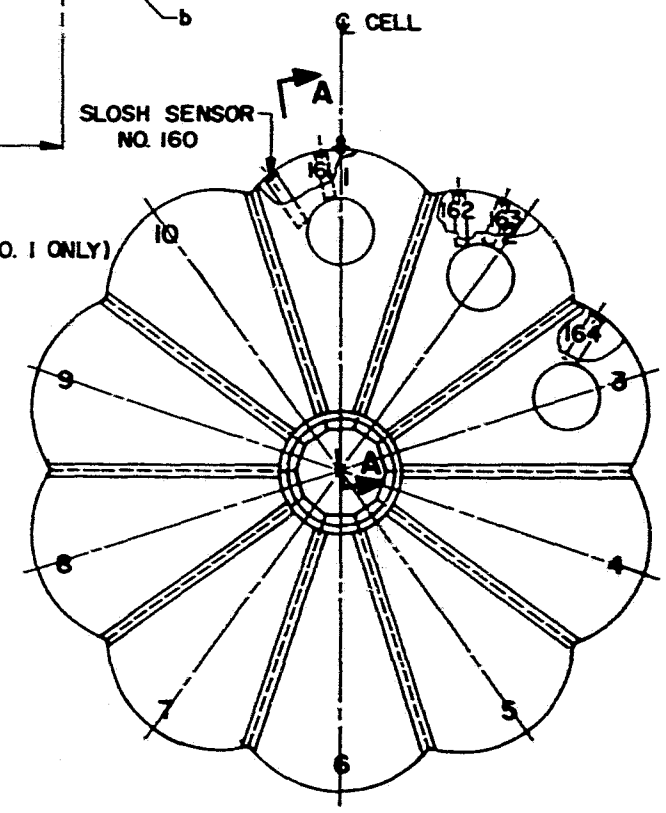


TOP VIEW OF MULTICELL TANK

FIGURE 2. INSTRUMENTATION (Sheet 1 of 2)

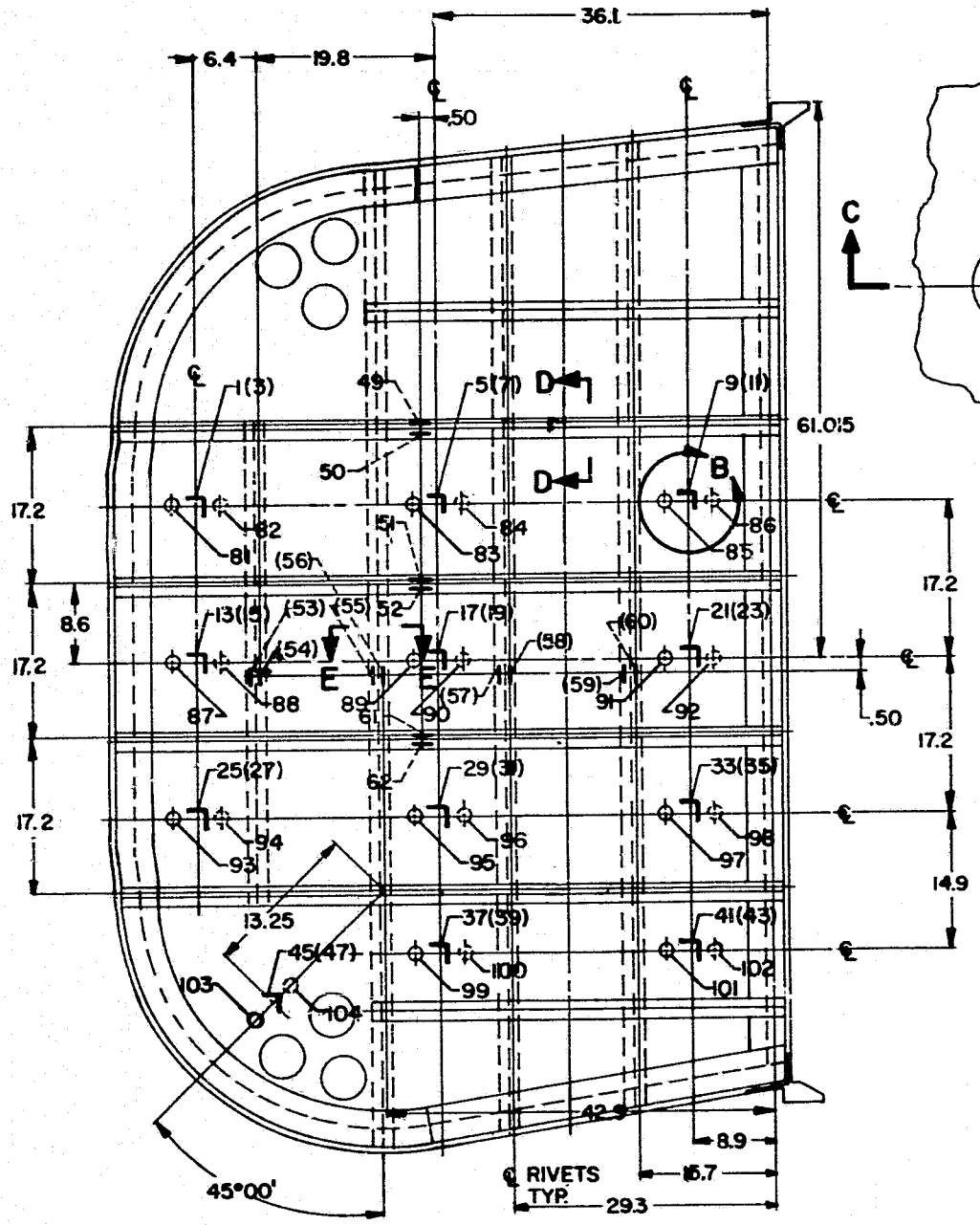


SECTION - AA

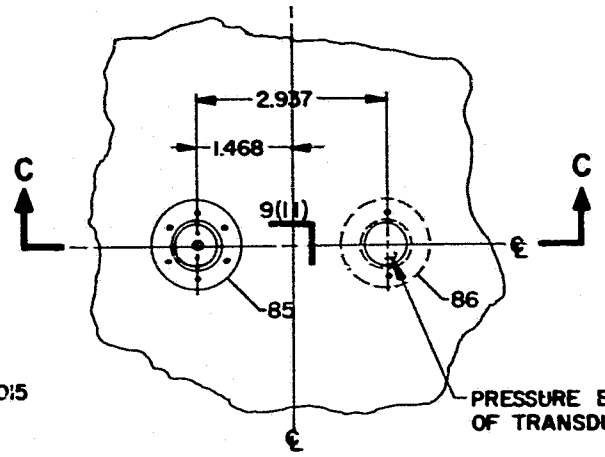


DETAIL "B"
TYPICAL 12 PLACES

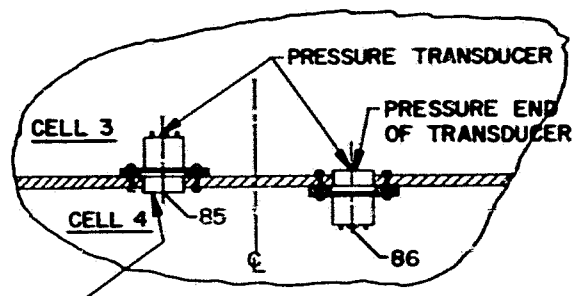


SECTION - CC

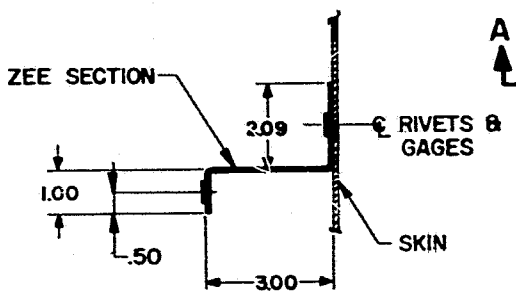


SECTION - DD
TYPICAL ALL HORIZONTAL WEB STIFFENERS

SECTION - EE
(ROTATED 90° CCW)
TYPICAL ALL VERTICAL WEB STIFFENERS

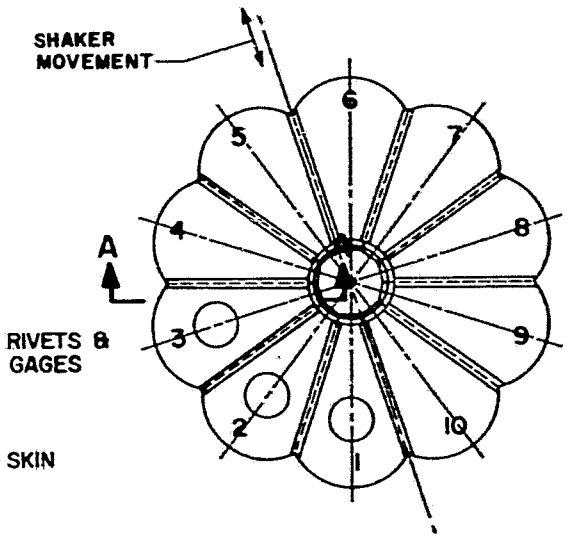


TOP VIEW OF MULTICELL TANK

FIGURE 2. INSTRUMENTATION (Sheet 2 of 2)

The amount of fluid required to fill the tank to the 1/2-full level is 25,423 liters (6716 gal.) and 38,134 liters (10,074 gal.) to the 3/4-full level.

2. Excitation Mode. Although there are four types of slosh excitation---translational, pitching, yawing, and rolling---it was concluded that for practical purposes the test should consist of translational excitation only. This translational excitation was originally planned for three cases: Case I, with the shaker force acting horizontally in the plane of the web between cell 1 and cell 10; Case II, with the shaker force acting horizontally along the bisector of the central angle of cell 1; Case III, with the shaker force acting horizontally in cell 1 in the vertical plane 28° from the web.

Case I was the only condition carried through; it is believed, however, that the data gathered from Case II and Case III would not have affected appreciably the conclusions presented in this report.

3. Oscillation Amplitude. The hydraulic shaker had a "range capability" from 0 to 6 inches displacement, double amplitude. In practice it was found that the smallest displacement which could be achieved was 0.07938 cm (0.03125 in.); this displacement was controlled by a coarse-resolution transducer which was used as a substitute for a fine resolution transducer unavailable at the time of the test. The upper limit of displacement, 3.81 cm (1.50 inch), was achieved without the irregularity of motion observed during small displacements (Fig.3).

4. Frequency and Force. The frequency range of the hydraulic shaker was from 0 to 20 cps, and the force capability ranged from 0 up to 22,680 Kg. (50 Kips).

5. Wave Measurement. Two techniques for measuring wave amplitude were proposed for the slosh test. The first technique consisted of the use of pressure transducers to measure differential head by differential pressures; the second called for the use of a variable-current-path resistance tape. The first technique was considered to be insufficiently sensitive for the head measurement of the small wave amplitudes which were anticipated. The second technique was adopted because it was sufficiently sensitive, and orientation presented no problems.

The second technique used a tape with a system of parallel wires (0.125 in. x 0.003 in. copper strands, flash coated with gold) to be fixed to the cell wall in a preselected location. The water in the cell served to complete the circuit between the wires. As a wave reached the tape, the crest and trough and all intermediate points caused a variable resistance in the system, proportional at any instant to the position of a particle on the wave. See Figure 4.

6. Splash Determination. Monitoring the incipient separation of a water droplet (impending splash criterion) from the wave crest was facilitated by the use of TV cameras. Later, a permanent film record

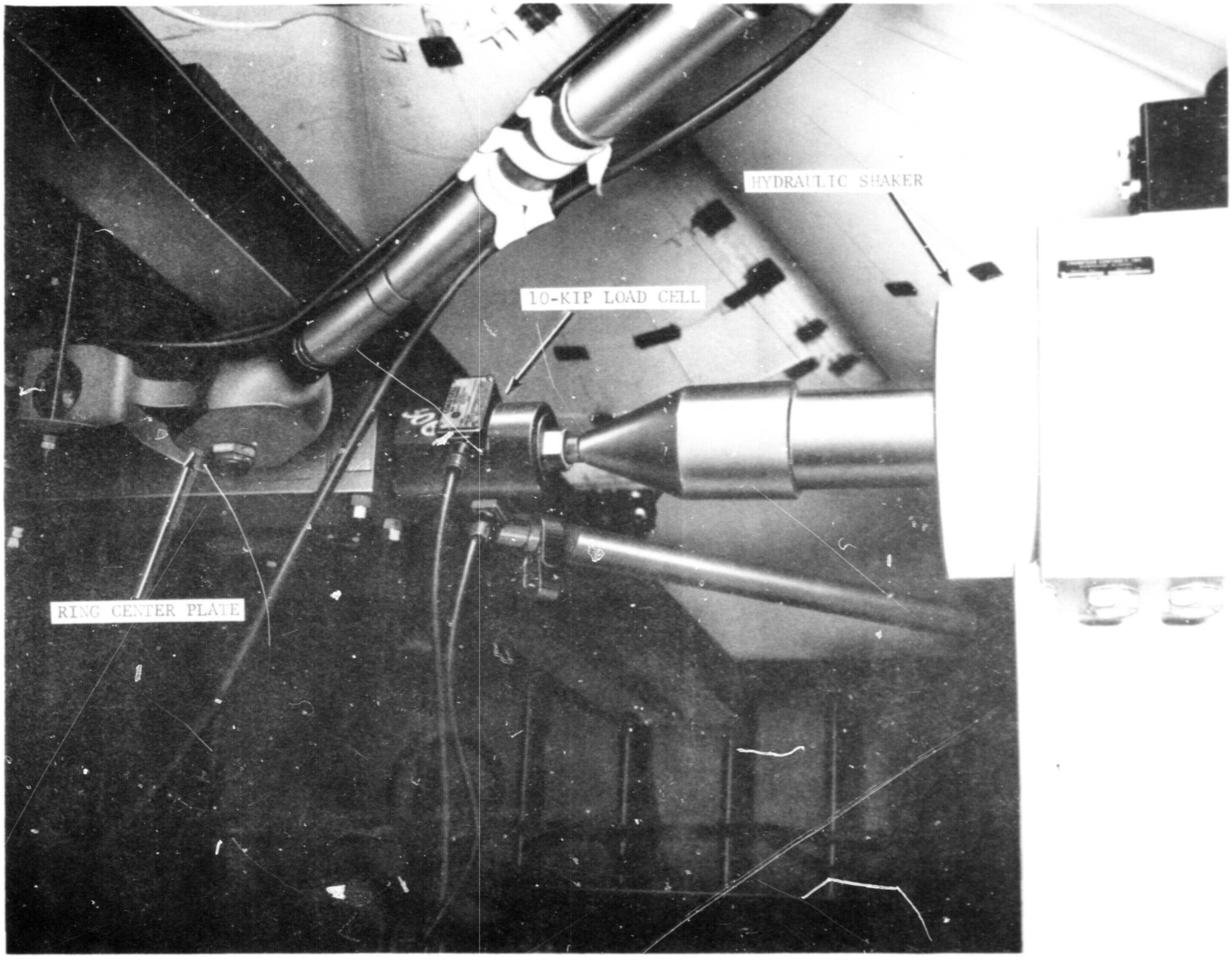


FIGURE 3. HYDRAULIC SHAKER

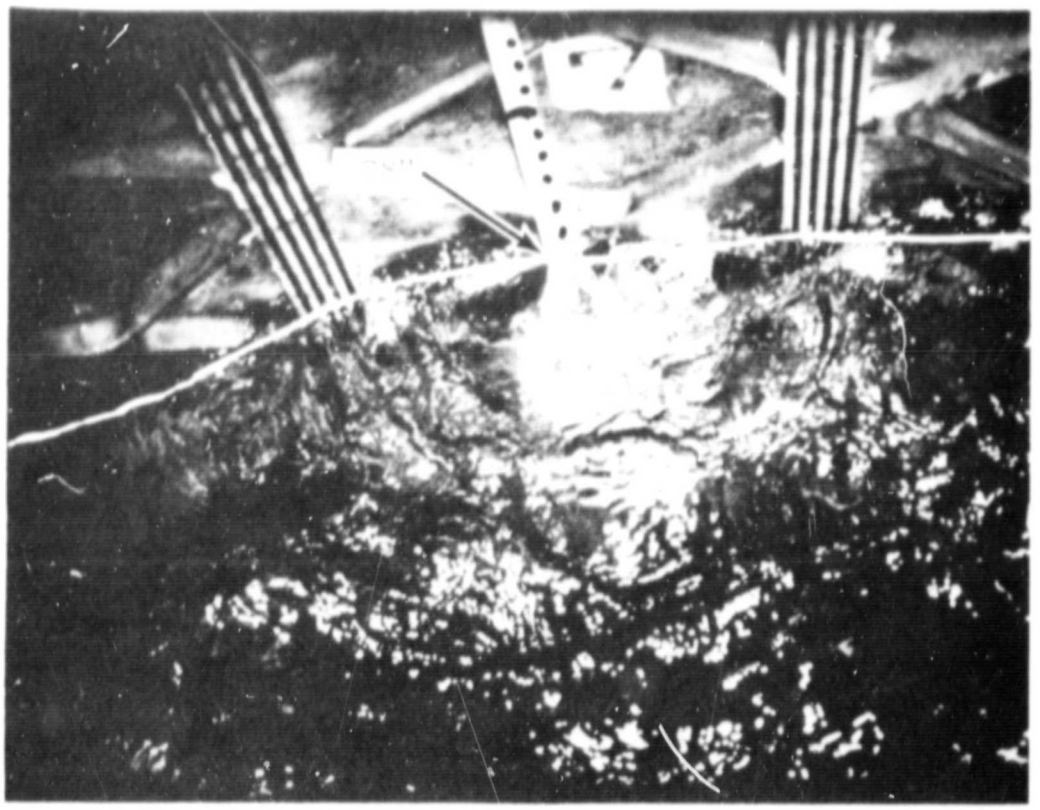

PEAK

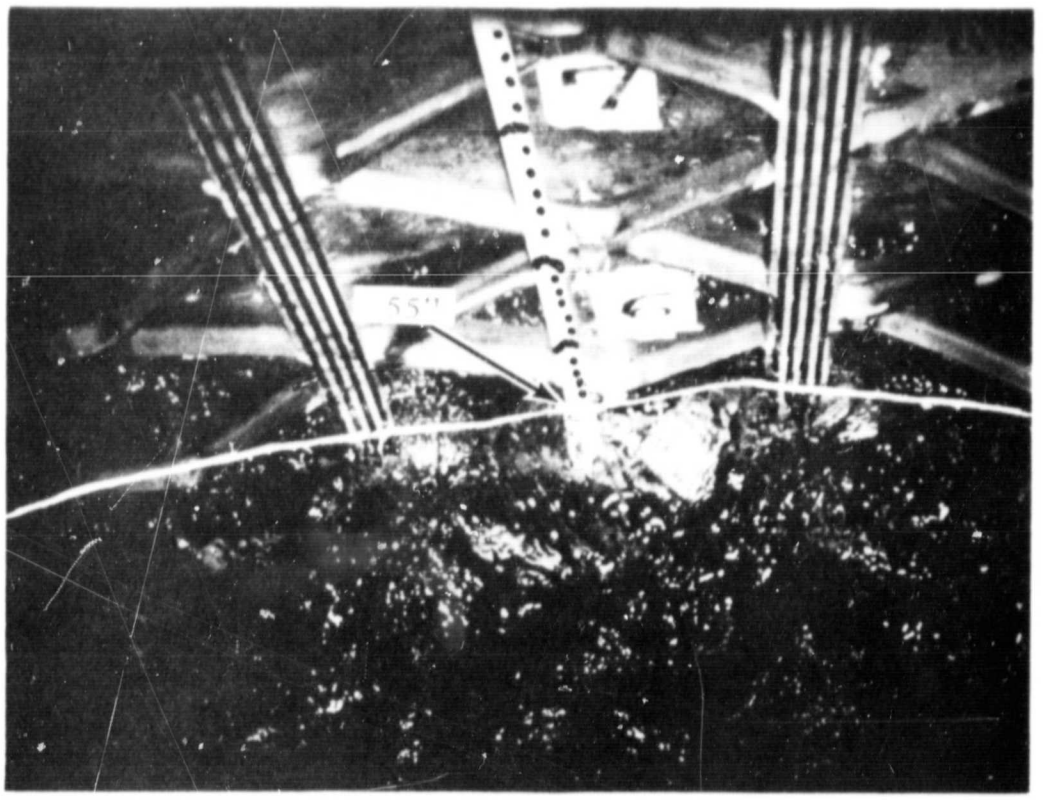

TROUGH

MAXIMUM NON-SPLASH SLOSH CONDITION
½ FULL WATER LEVEL

**FIGURE 4. WAVE FORMATION**

was made by movie cameras for the same operating conditions, and time-keyed. By the same token, the cessation of splash could also be determined. Further, movie film "stills" were helpful in verifying the maximum wave amplitudes; the verification was easily accomplished by observing the wave crest against the background of a white-faced steel tape which was fixed to an inside cell wall.

## SECTION IV. THEORETICAL BACKGROUND

### A. General

A theoretical analysis of liquid behavior in a tank with the geometry of the multicell was not available in the literature. Therefore, recourse was had to available analyses on tanks of geometry very similar to that of the multicell.

The annular-sector tank shown in Figure 5 has been used extensively for studies in the control of fuel sloshing. Therefore, theoretical expressions have been derived for natural frequencies, pressures, forces and moments, resulting from many types of tank excitation. (See References 3 and 4.)

To convert the multicell tank geometry to that of the annular-sector tank it was required to obtain an equivalent outer tank radius to replace the scollop of the multicell tank. This equivalent radius was determined by location of the center of gravity of the scolloped section. Thus, the equivalent annular-sector tank has the same cross sectional area as that of the existing multicell tank.

Even with this simplification, the theoretical expressions describing the slosh behavior for an annular-sector tank are very complex, and are lengthy to evaluate. After some investigation, it was decided that the inner radius of the annular tank could be neglected without significant error, since the ratio of inner radius to outer radius was quite small. It was determined from Reference 5 that this assumption would not appreciably affect the natural frequencies of the sloshing liquid for this geometry. This assumption greatly simplifies the expressions for natural frequencies pressures, forces and moments. These expressions, taken from Reference 3, for a sector tank (Figure 6) are given in Appendix A.

It was also required to determine an equivalent height of liquid in the circular cylindrical sectored tank, because of the complex geometry of the multicell bottom bulkhead. This equivalent height of liquid was determined by equating volumes in the multicell tank to the circular cylindrical sectored tank and solving for height of liquid. Thus, the geometry of the tanks shown in Figure 7 is used for the theoretical analysis which follows. It should be noted that for the 3/4-full condition, the static liquid level extended into the upper bulkhead of the multicell, thus requiring a modification of the equivalent radius.

### B. Natural Frequency

The equation for the natural frequencies of the sloshing liquid in a tenth-sector tank is

$$\omega_{mn}^2 = \frac{g}{a} \epsilon_{mn} \tanh\left(\epsilon_{mn} \frac{h}{a}\right)$$

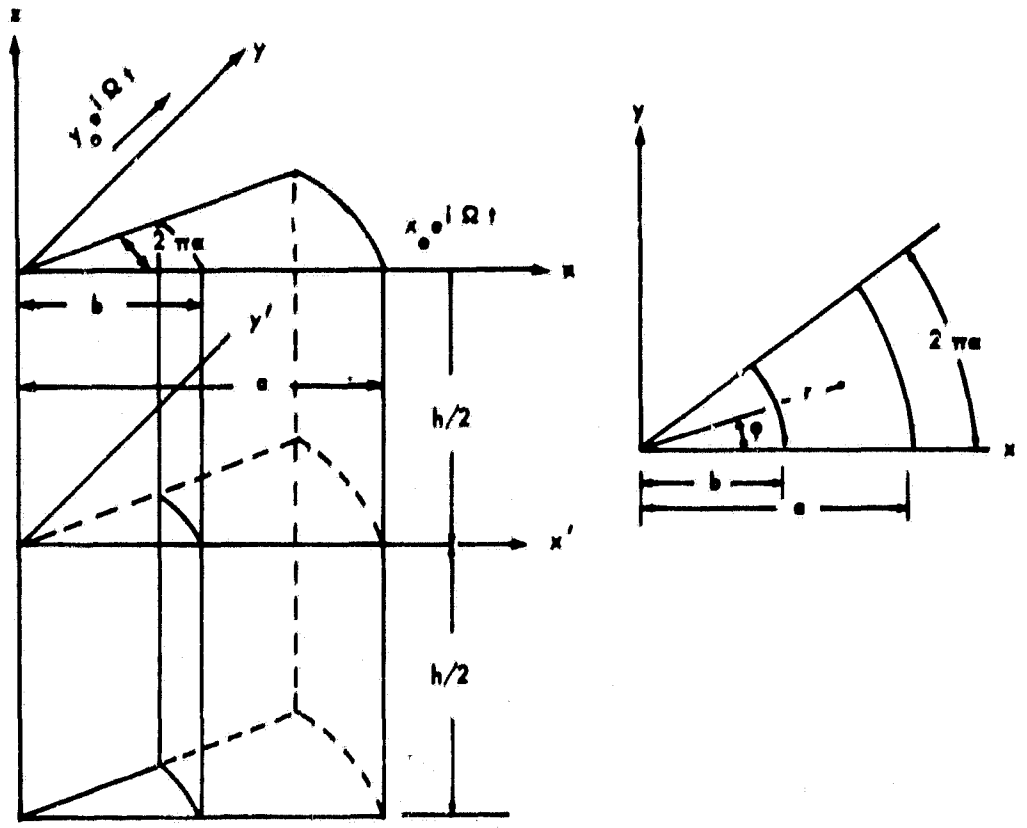


FIGURE 5. COORDINATE SYSTEM AND TANK GEOMETRY FOR ANNULAR-SECTOR TANK

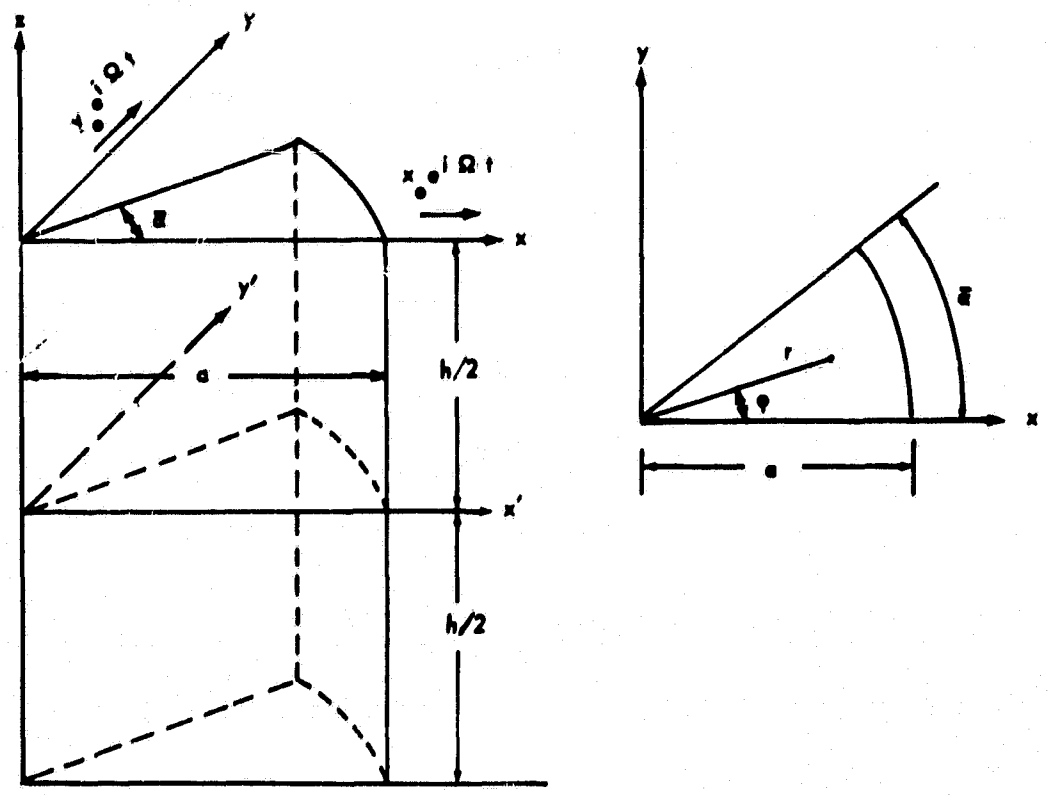


FIGURE 6. COORDINATE SYSTEM AND TANK GEOMETRY FOR TENTH-SECTOR TANK

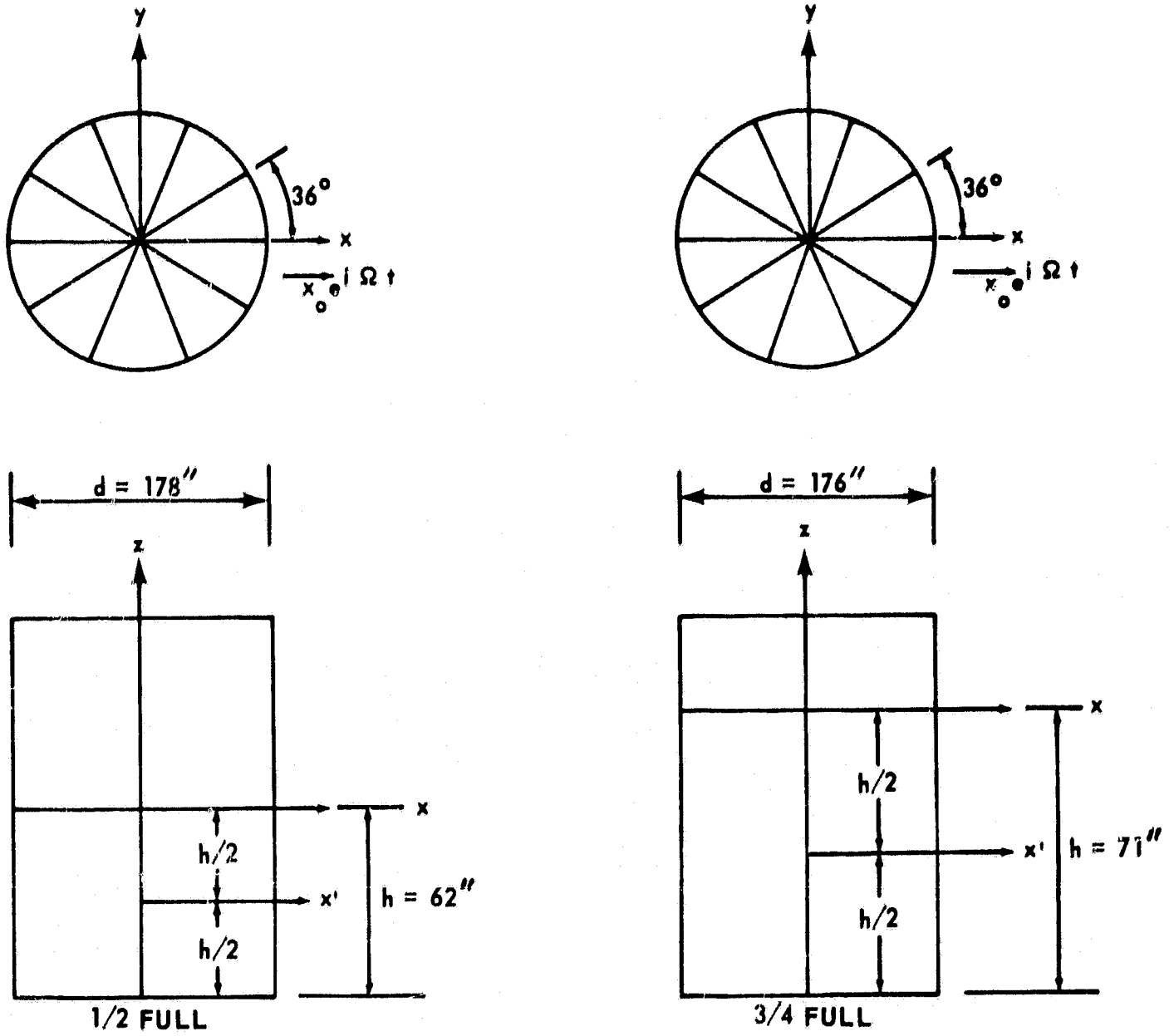


FIGURE 7. EQUIVALENT CIRCULAR CYLINDRICAL-SECTORED TANK

where the values of $\epsilon_{mn}$ are given in Appendix B for values of m and n. The subscripts m and n are integers ranging from 0 to $\infty$ and represent the mode shape of the liquid in the radial and tangential directions. The equation for the natural frequencies has been derived with the assumption of very small excitation amplitudes. As a consequence, the natural frequency of a tank under relatively large excitation amplitudes would not be in exact agreement with the expression above. A plot of the frequency equation versus liquid height ratio is shown in Figure 8 for the lowest three mode shapes, represented by values of $\epsilon_{mn}$. It can be seen from this plot that as h/a approaches 1.0 the value of the natural frequency approaches a constant value and remains constant for h/a greater than 1.0. The two vertical lines on this figure show the two values of h/a at which the multicell was tested. From their positions on the curves it can be seen that the lowest natural frequency for both test conditions should be nearly the same. Also, it is seen that natural frequency is independent of tank orientation or excitation.

## C. Pressure

The pressure at any point in the sectored tank shown in Figure 6 is

$$p = -g\rho t - \rho \frac{\partial \Phi}{\partial t} .$$

The first term is the pressure resulting from the static liquid and the second term is the pressure generated by the sloshing liquid (Ref. 3). Substitution of the velocity potential from Appendix A and differentiating with respect to t yields

$$p = -g\rho z - \sum_{m=0}^{\infty} \sum_{n=0}^{\infty} \rho \Omega^2 e^{i\Omega t} \begin{Bmatrix} x_o \\ y_o \end{Bmatrix} \left[ \begin{Bmatrix} r\cos\phi \\ r\sin\phi \end{Bmatrix} + \frac{b_{mn}\eta^2}{(1-\eta^2)} \begin{Bmatrix} a_m \\ c_m \end{Bmatrix} \cos 5m\phi \quad \frac{\cosh\left[\left(\frac{h}{a} + \frac{z}{a}\right)\epsilon_{mn}\right] J\left(\epsilon_{mn}\frac{r}{a}\right)}{\cosh\left(\epsilon_{mn}\frac{h}{a}\right)} \right].$$

This expression is for a single cell; however, the pressure at any point in any cell can be evaluated if the proper excitation amplitudes, ($X_o$ and $Y_o$) for that cell are used.

$$\omega_{mn}^2 = \frac{g}{a} \varepsilon_{mn} \tanh\left(\varepsilon_{mn} \frac{h}{a}\right)$$

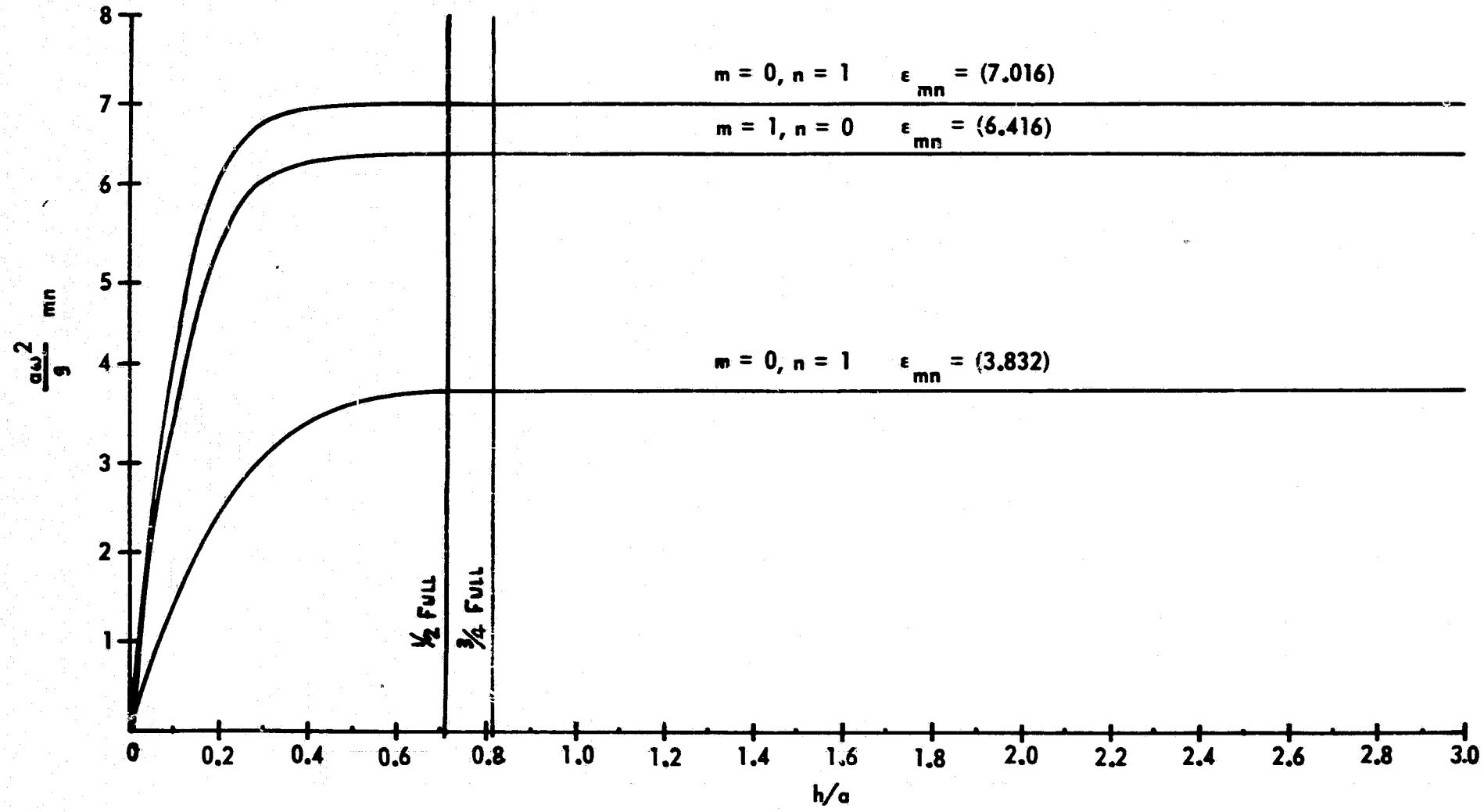


FIGURE 8. NATURAL FREQUENCY PARAMETER VERSUS FLUID HEIGHT RATIO FOR TENTH-SECTOR TANK

## D. Forces

The force expressions in Appendix A are only for a single sectored tank with local axis and excitation direction as shown in Figure 6. The total force generated by all the ten cells is required in order to correlate results obtained for the complete tank. Each cell of the complete tank has excitation amplitudes which are vectorial components of the total tank excitation amplitude. Thus, by taking each cell with its appropriate excitation amplitudes the resultant force in the x and y directions for each cell can be obtained. Then, by summation of the results from the ten cells, resultant forces can be obtained for the total tanks.

### 1. Force in x direction

The total force in the x direction for the complete tank due to lateral excitation as shown in Figure 7 is

$$(F_x)_{\text{Total}} = 2\Big[(F_x)_{x_o} + 2\cos^2 36^\circ (F_x)_{x_o} + 2\sin^2 36^\circ (F_y)_{y_o} + 2\cos^2 72^\circ (F_x)_{x_o} + 2\sin^2 72^\circ (F_y)_{y_o}\Big].$$

where

$$(F_x)_{x_o} = \frac{F_x}{x_o \rho a^3 e^{i\Omega t}} = \frac{\pi h}{10a}\Omega^2 \left[1 + \sum_{m=0}^{\infty}\sum_{n=0}^{\infty} \frac{10\sin\bar{\alpha}\, b_{mn}\eta^2}{\pi a(1-\eta^2)}\, a_m (-1)^{m+1}\, \frac{\tanh\kappa}{\kappa} \left\{ \frac{\bar{\alpha}^2}{(\pi^2 m^2 - \bar{\alpha}^2)}\, J(\epsilon_{mn}) + L_o(\epsilon_{mn}) \right\}\right].$$

and

$$(F_y)_{y_o} = \frac{F_y}{y_o \rho a^3 e^{i\Omega t}} = \frac{\pi h}{10a}\Omega^2 \left[1 - \sum_{m=0}^{\infty}\sum_{n=0}^{\infty} \frac{2 b_{mn}\eta^2 c_m}{\bar{\alpha} a(1-\eta^2)} \left[1 - (-1)^m \cos\bar{\alpha}\right] \frac{\tanh\kappa}{\kappa} \left\{ \frac{\bar{\alpha}^2}{(\pi^2 m^2 - \bar{\alpha}^2)}\, J(\epsilon_{mn}) + L_o(\epsilon_{mn}) \right\}\right].$$

2. Force in y direction

The total force in the y direction for the complete tank due to lateral excitation as shown in Figure 7 is

$$(F_y)_{\text{Total}} = 2\Big[(F_y)_{x_o} + 2\cos^2 36°\,(F_y)_{x_o} - 2\sin^2 36°\,(F_x)_{y_o} + 2\cos^2 72°\,(F_y)_{x_o} - 2\sin^2 72°\,(F_x)_{y_o}\Big].$$

where $$(F_y)_{x_o} = \frac{F_y}{x_o \rho a^3 e^{i\Omega t}} = -\frac{\pi h \Omega^2}{10a}\Bigg[$$

$$\sum_{m=0}^{\infty}\sum_{n=0}^{\infty}\frac{2b_{mn}\eta^2}{\bar{\alpha}\,a(1-\eta^2)}\,a_m\left[1 - (-1)^m\cos\bar{\alpha}\right]\frac{\tanh\kappa}{\kappa}\Bigg\{\frac{\bar{\alpha}^2}{(m^2\pi^2 - \bar{\alpha}^2)}\,J(\epsilon_{mn}) + L_o(\epsilon_{mn})\Bigg\}\Bigg].$$

and $$(F_x)_{y_o} = \frac{F_x}{y_o \rho a^3 e^{i\Omega t}} = \frac{\pi h}{10a}\Omega^2\Bigg[$$

$$\sum_{m=0}^{}\sum_{n=0}^{}\frac{10\sin\bar{\alpha}\;b_{mn}\eta^2}{\pi\,a(1-\eta^2)}\,c_m(-1)^{m+1}\,\frac{\tanh\kappa}{\kappa}\Bigg\{\frac{\bar{\alpha}^2}{(m^2\pi^2 - \bar{\alpha}^2)}\,J(\epsilon_{mn}) + L_o(\epsilon_{mn})\Bigg\}\Bigg].$$

## E. Moments

To obtain the total moment about the x' and y' axes due to the tank excitation shown in Figure 7 it will be required to sum expressions from the ten individual cells as was done for the force expressions in Section D. Therefore, with the basic expressions for a single cell given in Appendix A the total for the entire tank can be found.

1. Moment about x' axis

The total moment about the x' axis for the complete tank due to lateral excitation as shown in Figure 7 is

$$(M_x)_{total} = 2\Big[(M_x)_{x_o} + 2\cos^2 36^\circ (M_x)_{x_o} +$$

$$2\sin^2 36^\circ (M_y)_{y_o} + 2\cos^2 72^\circ (M_x)_{x_o} + 2\sin^2 72^\circ (M_y)_{y_o}\Big].$$

where
$$(M_x)_{x_o} = \frac{M_x}{x_o \rho a^4 e^{i\Omega t}} = -\frac{\pi h}{10a}\Omega^2 \left[\frac{a\sin^2\bar{\alpha}}{2h\bar{\alpha}} - \frac{b_{mn}\eta^2 a_m}{\bar{\alpha} a\ 1-\eta^2 \epsilon_{mn}}\right.$$

$$\left[1 - (-1)^m \cos\bar{\alpha}\right] \left\{\left[\frac{\bar{\alpha}^2}{(m^2\pi^2 - \bar{\alpha}^2)} J(\epsilon_{mn}) + L_o(\epsilon_{mn})\right]\right.$$

$$\left.\left[\tanh\kappa + \frac{2}{\kappa}\left(\frac{1}{\cosh\kappa} - 1\right)\right] + \frac{2\bar{\alpha}^2 \epsilon_{mn}^2 L_2(\epsilon_{mn})}{(m^2\pi^2 - \bar{\alpha}^2)\kappa\cosh\kappa}\right\}\Bigg].$$

and
$$(M_y)_{y_o} = \frac{M_y}{y_o \rho a^2 e^{i\Omega t}} = \frac{\pi h}{10a}\Omega^2 \left[\frac{4a\sin^2\bar{\alpha}}{h\bar{\alpha}} +\right.$$

$$\frac{\sin\bar{\alpha}\,(-1)^{m+1} b_{mn}\eta^2}{a\bar{\alpha}\,\epsilon_{mn}(1-\eta^2)} c_m \left\{\left[\frac{\bar{\alpha}^2}{(m^2\pi^2 - \bar{\alpha}^2)} J(\epsilon_{mn}) + L_o(\epsilon_{mn})\right]\right.$$

$$\left.\left.\left[\tanh\kappa + \frac{2}{\kappa}\left(\frac{1}{\cosh\kappa} - 1\right)\right] + \frac{2\bar{\alpha}^2 \epsilon_{mn}^2 L_2(\epsilon_{mn})}{(m^2\pi^2 - \bar{\alpha}^2)\kappa\cosh\kappa}\right\}\right].$$

2. Moment about y' axis

The total moment about the y' axis for the complete tank due to lateral excitation as shown in Figure 7 is

$$(M_y)_{total} = 2\Big[(M_y)_{x_o} + 2\cos^2 36°\,(M_y)_{x_o} - 2\sin^2 36°\,(M_x)_{y_o} + 2\cos^2 72°\,(M_y)_{x_o} - 2\cos^2 72°\,(M_x)_{y_o}\Big].$$

where

$$(M_y)_{x_o} = \frac{M_y}{x_o \rho a^4 e^{i\Omega t}} = \frac{\pi h}{10a}\Omega^2\left[\frac{4a}{h}\left(1 + \frac{\sin\bar{\alpha}\cos\bar{\alpha}}{\bar{\alpha}}\right) + \frac{\sin\bar{\alpha}\,(-1)^{m+1}\,b_{mn}\,\eta^2}{a\bar{\alpha}\,\epsilon_{mn}(1-\eta^2)}\,a_m\left\{\left[\frac{\bar{\alpha}^2}{(m^2\pi^2 - \bar{\alpha}^2)}\,J(\epsilon_{mn}) + L_o(\epsilon_{mn})\right]\left[\tanh\kappa + \frac{2}{\kappa}\left(\frac{1}{\cosh\kappa} - 1\right)\right] + \frac{2\bar{\alpha}^2\epsilon_{mn}^2 L_2(\epsilon_{mn})}{(m^2\pi^2 - \bar{\alpha}^2)\,\kappa\cosh\kappa}\right\}\right].$$

and

$$(M_x)_{y_o} = \frac{M_x}{y_o \rho a^4 e^{i\Omega t}} = -\frac{\pi h}{10a}\Omega^2\left[\frac{a}{4h}\left(1 - \frac{\sin\bar{\alpha}\cos\bar{\alpha}}{\bar{\alpha}}\right) - \frac{b_{mn}\eta^2\,c_m\left[1 - (-1)^m\cos\bar{\alpha}\right]}{\bar{\alpha}\,a\,(1-\eta^2)\,\epsilon_{mn}}\left\{\left[\frac{\bar{\alpha}^2}{(m^2\pi^2 - \bar{\alpha}^2}\,J(\epsilon_{mn}) + L_o(\epsilon_{mn})\right]\left[\tanh\kappa + \frac{2}{\kappa}\left(\frac{1}{\cosh\kappa} - 1\right)\right] + \frac{2\bar{\alpha}^2\,\epsilon_{mn}^2 L_2(\epsilon_{mn})}{(m^2\pi^2 - \bar{\alpha}^2)\,\kappa\cosh\kappa}\right\}\right].$$

## F. Surface Displacements

The displacement of any point on the surface in the sectored tank shown in Figure 6 is

$$\delta = -\frac{1}{g}\frac{\partial \Phi}{\partial t} .$$

Substitution of the velocity potential from Appendix A and differentiating with respect to t yields

$$\delta = \frac{\Omega^2 e^{i\Omega t}}{g} \left\{ \begin{matrix} x_c \\ y_o \end{matrix} \right\} \left[ \left\{ \begin{matrix} r\cos\phi \\ r\sin\phi \end{matrix} \right\} + \sum_{m=0}^{\infty} \sum_{n=0}^{\infty} \frac{b_{mn}\eta^2}{(1-\eta^2)} \left\{ \begin{matrix} a_m \\ c_m \end{matrix} \right\} \cos 5m\phi \; \frac{\cosh\left[\left(\frac{h}{a}+\frac{z}{a}\right)\epsilon_{mn}\right] J\left(\epsilon_{mn}\frac{r}{a}\right)}{\cosh\left(\epsilon_{mn}\frac{h}{a}\right)} \right] .$$

This expression is for a single cell, but it can be evaluated for any cell if the proper excitation amplitudes for that cell are used.

## SECTION V. TEST EVALUATION

This section contains the evaluation of the theoretical expressions for frequency, force, moment, pressure, etc., obtained in Section IV for the geometry given in Figure 7.

Correlation of experimental results with theory is then made.

### A. Natural Frequency

The theoretical expression for the natural frequency of the sloshing liquid in a tenth-sector tank,as given in Section IV-C, is independent of excitation amplitude. The experimental determination of liquid natural frequency must, however, be done by tank excitation and frequency variation to obtain the transition from stable to unstable sloshing which determines the experimental value of natural frequency. However, experimental studies have failed to yield very good agreement between measured and predicted liquid frequencies (Ref. 3), the measured frequencies always being somewhat low.

This "softening" characteristic is a consequence of the essentially nonlinear behavior of compartmented tanks.

It was revealed that there was a strong dependence of the liquid frequencies on excitation amplitude and this indicated agreement with the theoretical values for vanishingly small excitation amplitudes. This effect has been shown in Reference 3.

The theoretical expression for frequency can be rewritten in nondimensional form as

$$\frac{d}{g}\,\omega_{mn}^2 = 2\,\epsilon_{mn}\tanh\left(\epsilon_{mn}\,\frac{h}{a}\right)$$

When this parameter is plotted versus the ratio of excitation amplitude to tank diameter ($x_o/d$) the results are as shown in Figure 8 for the first two values of natural frequency.

The experimental values of natural frequency obtained for cells 1, 2, and 3 as given in Tables I and II were plotted on Figure 9 at the appropriate excitation amplitude parameter from which they were obtained. Results from sectored tanks (Ref. 3) have shown that, at higher $X_o/d$ ratios, natural frequency parameters were further below theoretical values than those obtained at lower $x_o/d$ ratios. This trend cannot be established for this test because of the small number of data points.

It can also be seen from Figure 9 that,for this tank excitation, cell 1 is sloshing in the first natural frequency while cells 2 and 3 are sloshing in the second natural frequency. This occurs because of the geometrical orientation of the cells with respect to tank excitation. The radial type mode shape associated with the first natural

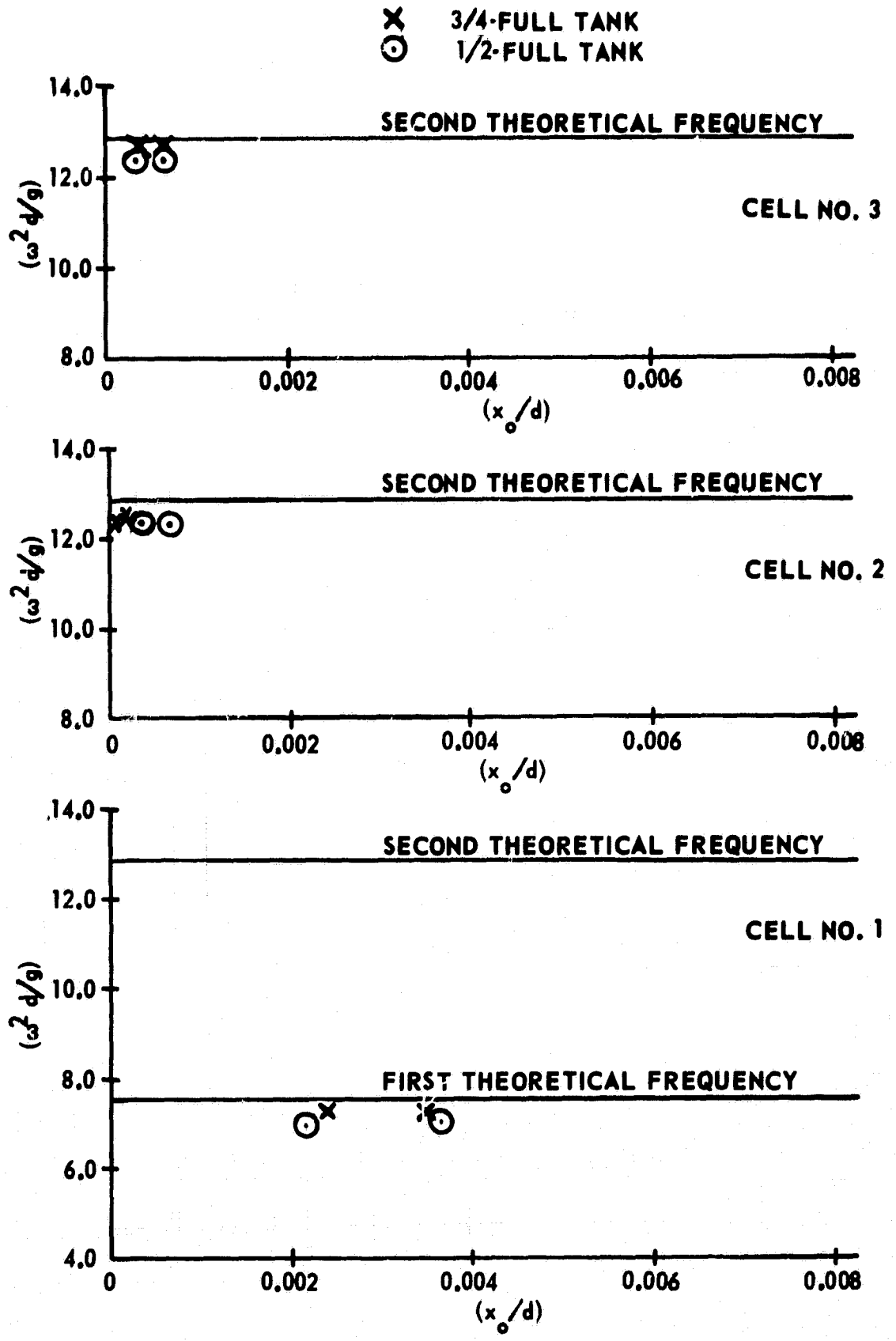


FIGURE 9. FREQUENCY PARAMETER VERSUS EXCITATION AMPLITUDE PARAMETER

frequency occurs in cell 1 because the tank excitation is also radial for that cell. However, for cells 2 and 3 the tank excitation is generally tangential, thus exciting the tangential mode shape associated with the second natural frequency. These mode shapes can be seen in photographs taken from the television camera data. See Figure 4.

For the 1/2-full tank the first two values of theoretical natural frequency are

$$f_{00} = \omega_{00}/2\pi = 0.643 \text{ hertz}$$

$$f_{10} = \omega_{10}/2\pi = 0.839 \text{ hertz}$$

and for the 3/4-full tank the first two values of theoretical natural frequency are

$$f_{00} = 0.646 \text{ hertz}$$

$$f_{10} = 0.845 \text{ hertz}$$

Comparison of these values with those obtained experimentally and listed in Tables I and II shows good agreement, especially at low excitation amplitude.

## B. Lateral Forces

The theoretical expressions for total tank force in the x and y directions obtained in Section IV-D were evaluated using appropriate geometric parameters for the 1/2-full and 3/4-full test conditions and the values given in Appendix B. Plots were then made of the force expressions versus values of tank forcing frequency ( $\Omega$ ). These plots are shown in Figures 10, 11, 12,and 13 for force in the x and y directions for both 1/2-and 3/4-full test conditions. The range of forcing frequency plotted included the two lowest liquid natural frequencies; these are indicated by the two broken vertical lines.

The total tank force in the x direction was measured experimentally by a load cell connecting the mounting ring and the shaker rod which excited the tank. These forces, for particular conditions of sloshing in the three cells, are tabulated in Tables I and II under the heading of L.C. output. There was no method provided to measure tank force in the y direction.

The experimentally measured values of force in the x direction for both the 1/2- and 3/4-full test conditions were nondimensionalized by appropriate parameters, and the results plotted as points on Figures 10 and 11. Several load cell readings indicated a range of values during the test (Refer to Tables I and II.) An average reading was plotted for these cases.

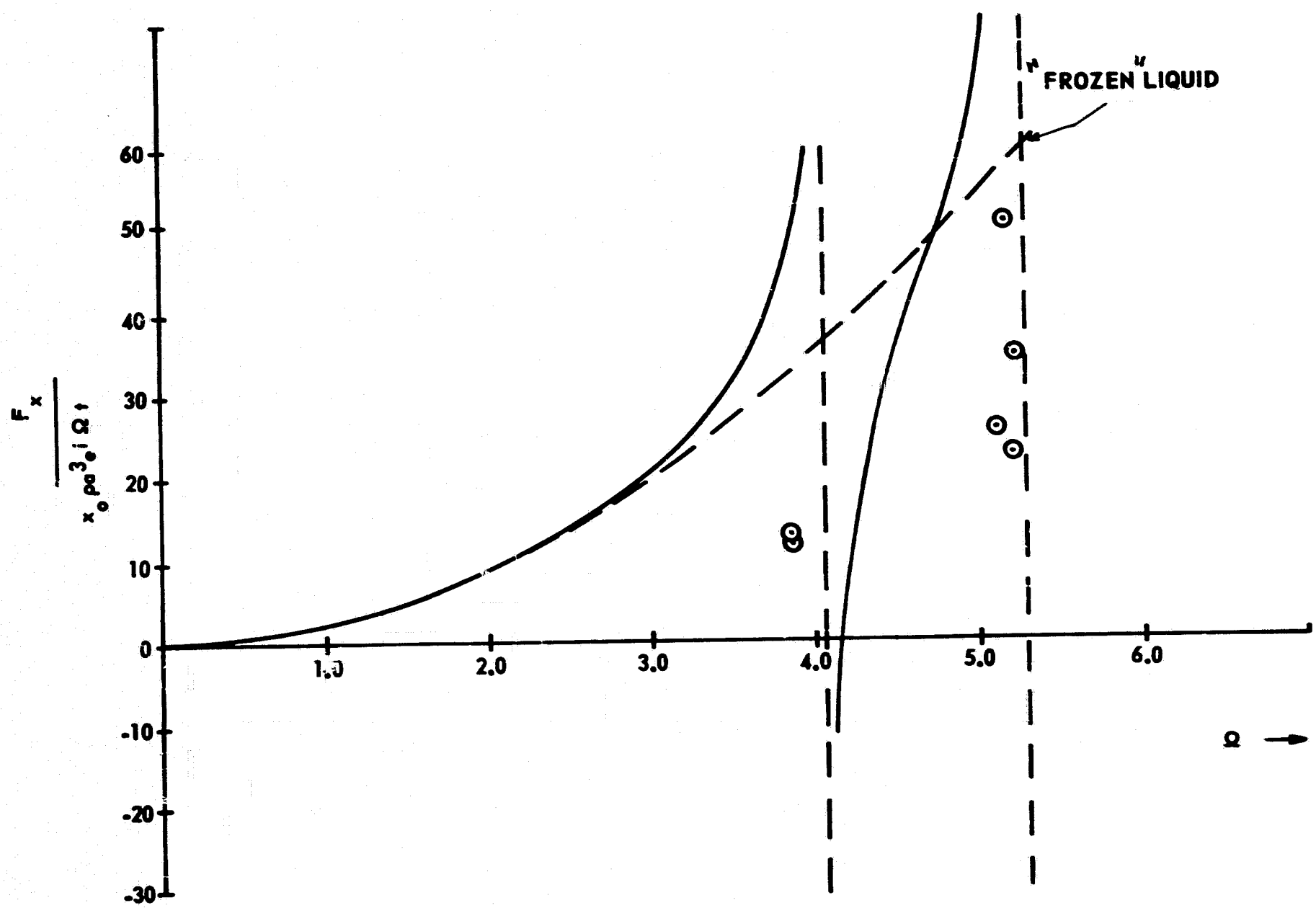


FIGURE 10. FORCE IN X DIRECTION FOR 1/2-FULL TANK VERSUS FORCING FREQUENCY

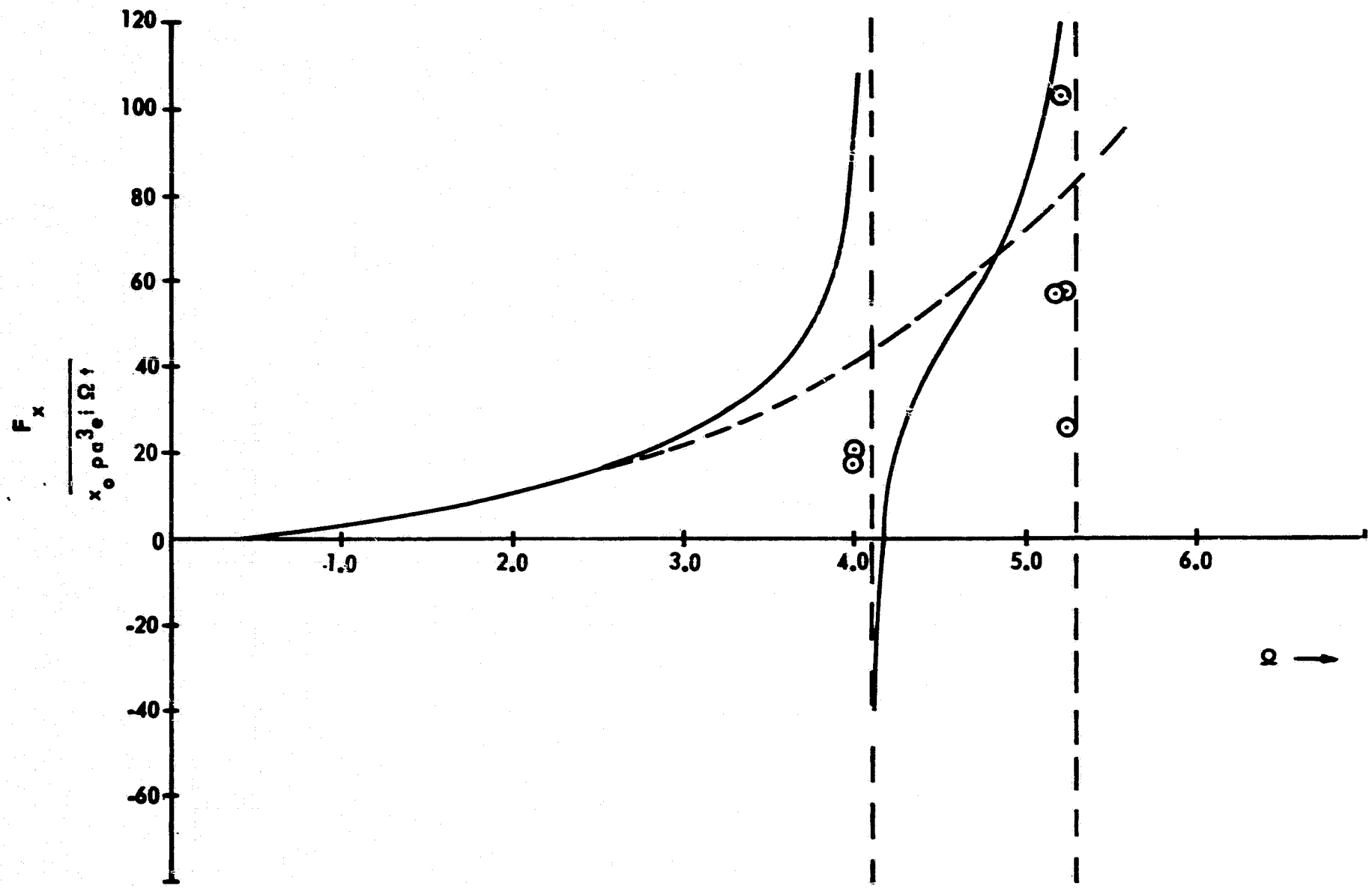


FIGURE 11. FORCE IN X DIRECTION FOR 3/4-FULL TANK VERSUS FORCING FREQUENCY

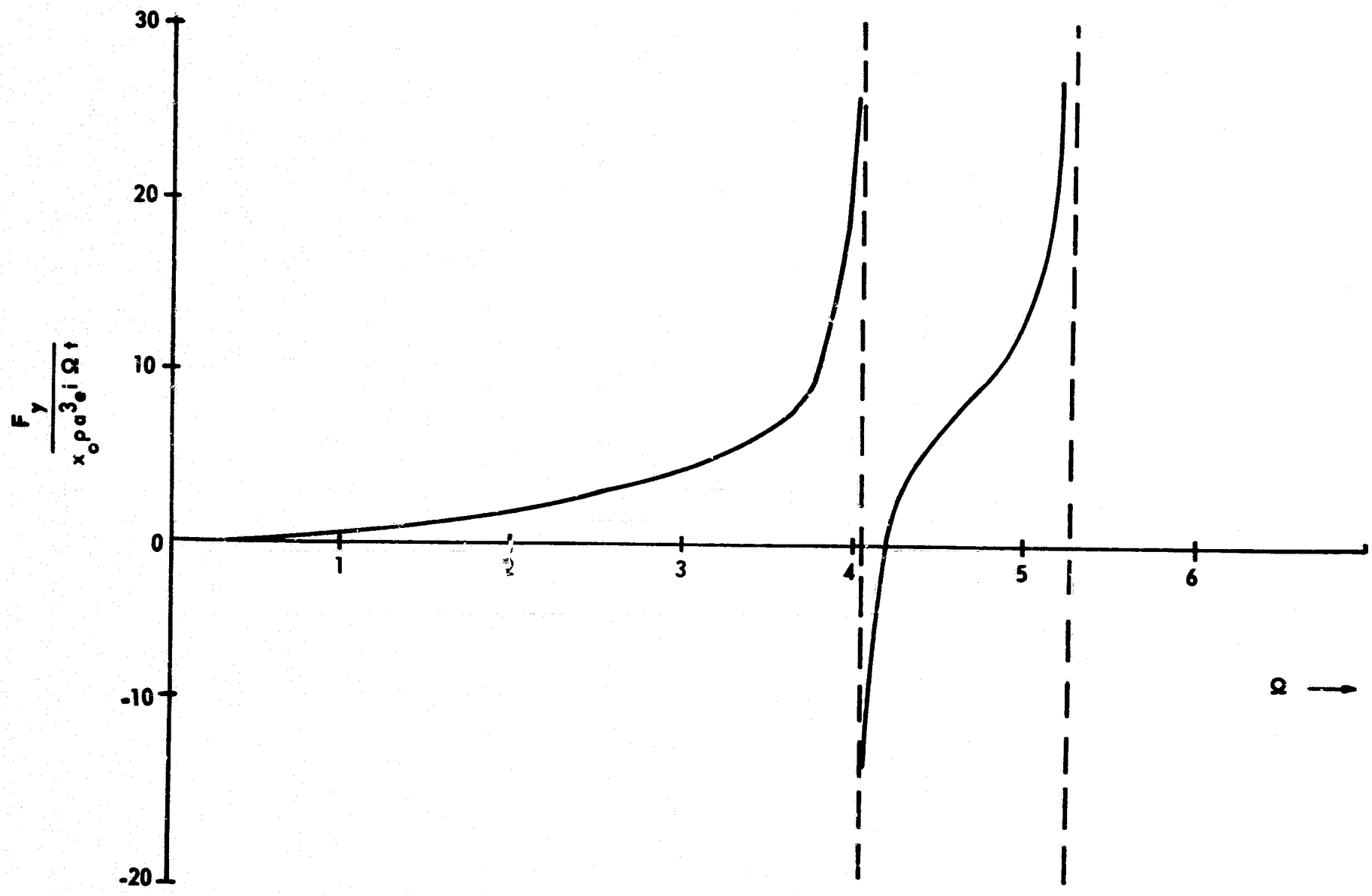


FIGURE 12. FORCE IN Y DIRECTION FOR 1/2-FULL TANK VERSUS FORCING FREQUENCY

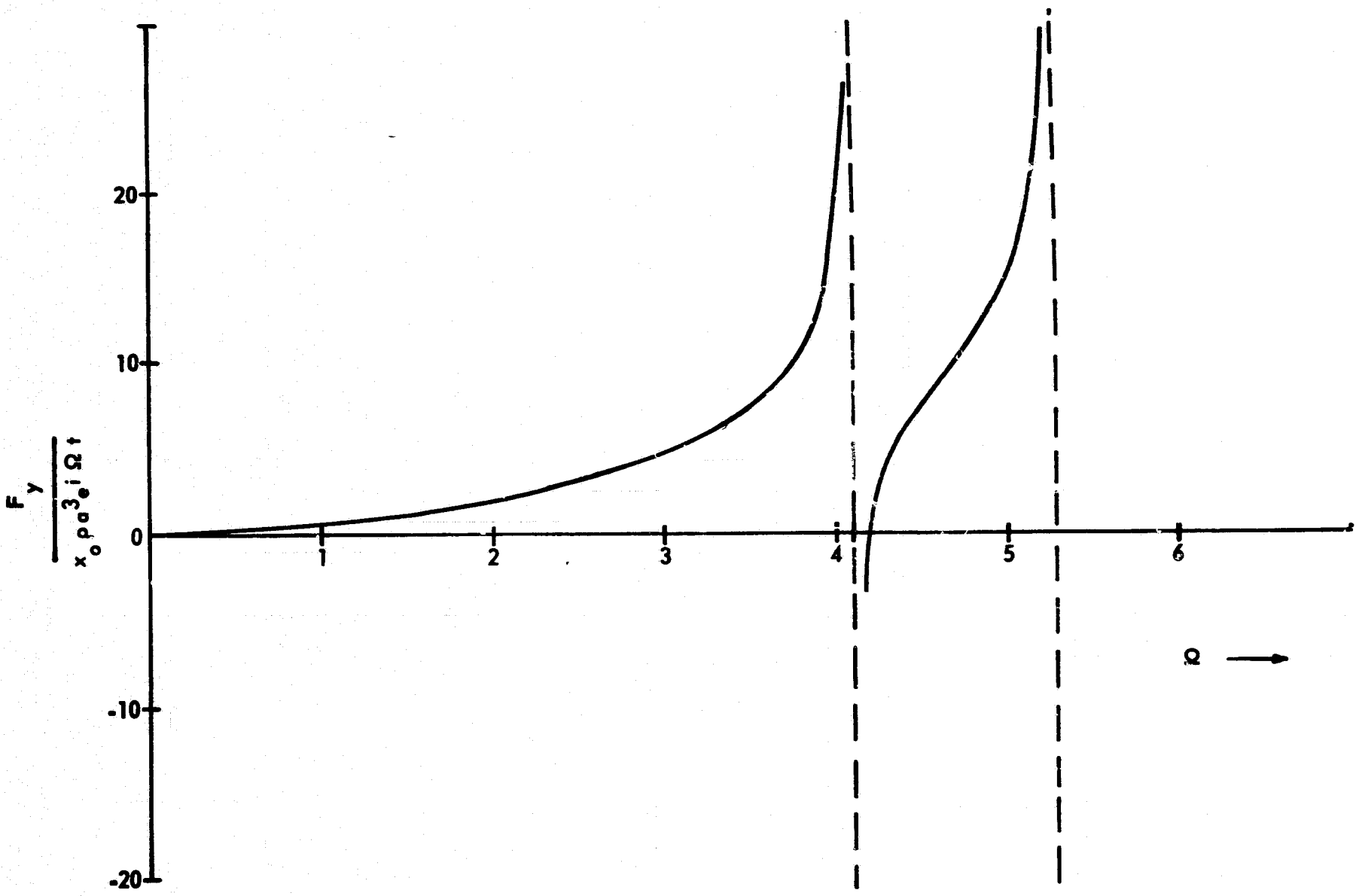


FIGURE 13. FORCE IN Y DIRECTION FOR 3/4-FULL TANK VERSUS FORCING FREQUENCY

**Table I.**

**Transducer Output When Tank is ½ Full**

| | CELL 1 | | CELL 2 | | CELL 3 | |
|---|---|---|---|---|---|---|
| R.F. | .613 Hz | .615 Hz | .820 Hz | .815 Hz | .825 Hz | .827 Hz |
| S.D. | .850 in. | 1.425 in. | .124 in. | .239 in. | .128 in. | .244 in. |
| GAGE | μ - in. | μ - in. | μ - in. | μ - in. | μ - in. | μ - in. |
| 1 | * | * | * | * | * | * |
| 2 | * | * | * | * | * | * |
| 3 | * | * | * | * | * | * |
| 4 | 0 | 0 | 0 | 0 | 0 | 0 |
| 5 | 0 | 0 | 0 | 0 | 0 | 0 |
| 6 | 0 | 0 | 0 | 0 | 0 | 0 |
| 7 | 0 | 0 | 0 | 0 | 0 | 0 |
| 8 | 0 | 0 | 0 | 0 | 0 | 0 |
| 9 | 0 | 0 | 0 | 0 | 0 | 0 |
| 10 | 0 | 0 | 0 | 0 | 0 | 0 |
| 11 | * | * | * | * | * | * |
| 12 | * | * | * | * | * | * |
| 13 | 0 | 160 | 400 | 400 | 320 | 400 |
| 14 | 280 | 330 | 665 | 780 | 665 | 780 |
| 15 | 0 | 0 | 800 | 800 | 0 | 0 |
| 16 | 0 | 0 | 330 | 265 | 0 | 330 |
| 17 | 210 | 250 | 250 | 210 | 250 | 250 |
| 18 | 220 | 220 | 180 | 180 | 180 | 145 |
| 19 | * | * | * | * | * | * |
| 20 | 0 | 0 | 0 | 0 | 0 | 0 |
| 21 | * | * | * | * | * | * |
| 22 | 400 | 400 | 0 | 0 | 0 | 0 |
| 23 | * | * | * | * | * | * |
| 24 | * | * | * | * | * | * |
| 25 | 0 | 0 | 600 | 600 | 600 | 600 |
| 26 | * | * | * | * | * | * |
| 27 | 0 | 0 | 0 | 0 | 0 | 0 |
| 28 | 0 | 0 | 0 | 0 | 0 | 0 |
| 29 | 0 | 0 | 0 | 0 | 0 | 0 |
| 30 | 0 | 0 | 0 | 0 | 0 | 0 |
| 31 | 100 | 165 | 0 | 0 | 0 | 0 |
| 32 | 0 | 0 | 0 | 0 | 0 | 0 |
| 33 | 350 | 350 | 0 | 0 | 0 | 0 |
| 34 | 85 | 200 | 0 | 0 | 0 | 0 |
| 35 | 200 | 290 | 0 | 0 | 0 | 0 |

**SYMBOLS:** R.F. = Resonant Frequency
S.D. = Shaker Displacement
μ = Micro
* = Bad Gage

**Table I. (Continued)**

**Transducer Output When Tank is ½ Full**

| | CELL 1 | | CELL 2 | | CELL 3 | |
|---|---|---|---|---|---|---|
| R.F. | .613 Hz | .615 Hz | .820 Hz | .815 Hz | .825 Hz | .827 Hz |
| S.D. | .850 in. | 1.425 in. | .124 in. | .239 in. | .128 in. | .244 in. |
| GAGE | μ - in. | μ - in. | μ - in. | μ - in. | μ - in. | μ - in. |
| 36 | 0 | 160 | 0 | 0 | 0 | 0 |
| 37 | 0 | 0 | 0 | 0 | 0 | 0 |
| 38 | 0 | 90 | 0 | 0 | 0 | 0 |
| 39 | * | * | * | * | * | * |
| 40 | * | * | * | * | * | * |
| 41 | 0 | 0 | 0 | 0 | 0 | 0 |
| 42 | 0 | 0 | 0 | 0 | 0 | 0 |
| 43 | 0 | 0 | 0 | 0 | 0 | 0 |
| 44 | 0 | 0 | 0 | 0 | 0 | 0 |
| 45 | 0 | 0 | 0 | 0 | 0 | 0 |
| 46 | * | * | * | * | * | * |
| 47 | * | * | * | * | * | * |
| 48 | 0 | 0 | 0 | 0 | 0 | 0 |
| 49 | 0 | 0 | 0 | 0 | 0 | 0 |
| 50 | * | * | * | * | * | * |
| 51 | 0 | 0 | 0 | 0 | 0 | 0 |
| 52 | * | * | * | * | * | * |
| 53 | 145 | 170 | 170 | 285 | 170 | 230 |
| 54 | 0 | 0 | 0 | 0 | 0 | 0 |
| 55 | 265 | 315 | 210 | 315 | 210 | 265 |
| 56 | 0 | 0 | 0 | 0 | 0 | 0 |
| 57 | 345 | 455 | 230 | 285 | 145 | 285 |
| 58 | 0 | 0 | 0 | 0 | 0 | 0 |
| 59 | * | * | * | * | * | * |
| 60 | * | * | * | * | * | * |
| 61 | 0 | 0 | 0 | 0 | 0 | 0 |
| 62 | * | * | * | * | * | * |
| 67 | 0 | 0 | 0 | 0 | 0 | 0 |
| 68 | 0 | 0 | 0 | 0 | 0 | 0 |
| 69 | 0 | 0 | 0 | 0 | 0 | 0 |
| 70 | 0 | 0 | 0 | 0 | 0 | 0 |
| 71 | 0 | 0 | 0 | 0 | 0 | 0 |
| 72 | 0 | 0 | 0 | 0 | 0 | 0 |
| 73 | 0 | 0 | 0 | 0 | 0 | 0 |
| 74 | 0 | 0 | 0 | 0 | 0 | 0 |

**SYMBOLS:** R.F. = Resonant Frequency
S.D. = Shaker Displacement
μ = Micro
* = Bad Gage

**Table I. (Concluded)**

**Transducer Output When Tank is ½ Full**

| | CELL 1 | | CELL 2 | | CELL 3 | |
|---|---|---|---|---|---|---|
| R.F. | .613 Hz | .615 Hz | .820 Hz | .815 Hz | .825 Hz | .827 Hz |
| S.D. | .850 in. | 1.425 in. | .124 in. | .239 in. | .128 in. | .244 in. |
| P.T. | psi | psi | psi | psi | psi | psi |
| 81 | * | * | * | * | * | * |
| 82 | 0 | 0 | 0 | 0 | 0 | 0 |
| 83 | 0 | 0 | 0 | 0 | 0 | 0 |
| 84 | * | * | * | * | * | * |
| 85 | 0 | .30 | 0 | 0 | 0 | 0 |
| 86 | 0 | 0 | 0 | 0 | 0 | 0 |
| 87 | * | * | * | * | * | * |
| 88 | * | * | * | * | * | * |
| 89 | .35 | .50 | .20 | .25 | .20 | .25 |
| 90 | * | * | * | * | * | * |
| 91 | .35 | .35 | .03 | .05 | .03 | .08 |
| 96 | 0 | .10 | 0 | 0 | 0 | 0 |
| 99 | .02 | .06 | 0 | 0 | 0 | 0 |
| 100 | * | * | * | * | * | * |
| 104 | 0 | 0 | 0 | 0 | 0 | 0 |
| 105 | 0 | 0 | 0 | 0 | 0 | 0 |
| 106 | .35 | .35 | 0 | 0 | 0 | 0 |

| S.S.† | Oscillograph Movement and Corresponding (Peak-to-Trough Slosh Movement) (Inches) | | | | | |
|---|---|---|---|---|---|---|
| 160 | .375(9¼) | .450(15½) | .140(N.A.) | .225(N.A.) | .180(N.A.) | .300(N.A.) |
| 162 | .275(N.A.) | .360(N.A.) | .230(10 3/4) | .300(14¼) | .200(N.A.) | .300(N.A.) |
| 164 | .080(N.A.) | .140(N.A.) | .580(N.A.) | .625(N.A.) | .560(11) | .650(14) |

| L.F. | Change in Load While Sloshing (Pounds) (Peak Load-Minimum Load) | | | | | |
|---|---|---|---|---|---|---|
| 1 | 1560 | 2380-2630 | 560-715 | 750-935 | 435-680 | 620-865 |
| 2 | 910-1210 | 1520-1670 | 455-530 | 530-605 | 304-450 | 420-610 |
| 3 | 190 | 250 | 60-95 | 125 | 95-125 | 155 |
| 4 | 805-895 | 1070-1340 | 585-675 | 535-715 | 405-675 | 585-810 |
| 5 | 1435 | 2375-2500 | 310-465 | 750 | 280-435 | 650-710 |
| 6 | * | * | * | * | * | * |
| 7 | 690-940 | 1060-1250 | 370-560 | 625-750 | 435-650 | 590-745 |
| 8 | 810 | 1375-1440 | 250-340 | 435 | 185-280 | 370-465 |
| 9 | 950 | 1300 | 375 | 500 | 250-600 | 375-500 |
| 10 | 600 | 950 | 350 | 500 | 250-450 | 450-575 |
| L.C. | 720 | 1040 | 415 | 400 | 200-390 | 280-460 |

SYMBOLS: R.F. = Resonant Frequency
S.D. = Shaker Displacement
P.T. = Pressure Transducer
N.A. = Not Available
S.S. = Slosh Sensor
L.F. = Load Feet
L.C. = Load Cell
* = Bad Gage

†NOTE: The actual slosh movement is not linearly proportional to oscillograph movement.

**Table II.**

**Transducer Output When Tank is ¾ Full**

| | CELL 1 | | CELL 2 | | CELL 3 | |
|---|---|---|---|---|---|---|
| R.F. | .634 Hz | .633 Hz | .830 Hz | .830 Hz | .840 Hz | .840 Hz |
| S.D. | .850 in. | 1.250 in. | .034 in. | .067 in. | .129 Hz | .222 in. |
| GAGE | μ - in. | μ - in. | μ - in. | μ - in. | μ - in. | μ - in. |
| 1 | * | * | * | * | * | * |
| 2 | * | * | * | * | * | * |
| 3 | * | * | * | * | * | * |
| 4 | 0 | 0 | 0 | 0 | 0 | 0 |
| 5 | 0 | 0 | 0 | 0 | 0 | 0 |
| 6 | 0 | 0 | 0 | 0 | 0 | 0 |
| 7 | 0 | 0 | 0 | 0 | 0 | 0 |
| 8 | 300 | 350 | 0 | 0 | 0 | 0 |
| 9 | 240 | 240 | 0 | 0 | 0 | 0 |
| 10 | 0 | 0 | 0 | 0 | 0 | 0 |
| 11 | * | * | * | * | * | * |
| 12 | * | * | * | * | * | * |
| 13 | 0 | 0 | 0 | 0 | 0 | 0 |
| 14 | 0 | 0 | 0 | 0 | 0 | 0 |
| 15 | 0 | 0 | 0 | 0 | 0 | 0 |
| 16 | 0 | 0 | 0 | 0 | 0 | 0 |
| 17 | 320 | 720 | 0 | 0 | 0 | 240 |
| 18 | 200 | 275 | 0 | 75 | 75 | 125 |
| 19 | * | * | * | * | * | * |
| 20 | 0 | 0 | 0 | 0 | 0 | 0 |
| 21 | * | * | * | * | * | * |
| 22 | 0 | 200 | 0 | 0 | 0 | 0 |
| 23 | * | * | * | * | * | * |
| 24 | * | * | * | * | * | * |
| 25 | 0 | 0 | 0 | 0 | 0 | 0 |
| 26 | * | * | * | * | * | * |
| 27 | 80 | 180 | 0 | 0 | 0 | 100 |
| 28 | 0 | 0 | 0 | 0 | 0 | 0 |
| 29 | 0 | 0 | 0 | 0 | 0 | 0 |
| 30 | 0 | 0 | 0 | 0 | 0 | 0 |
| 31 | 135 | 335 | 0 | 0 | 0 | 0 |
| 32 | 0 | 0 | 0 | 0 | 0 | 0 |
| 33 | 0 | 150 | 0 | 0 | 0 | 100 |
| 34 | 55 | 170 | 0 | 0 | 0 | 70 |
| 35 | 215 | 400 | 0 | 55 | 55 | 145 |

SYMBOLS: R.F. = Resonant Frequency
S.D. = Shaker Displacement
μ = Micro
* = Bad Gage

**Table II. (Continued)**

**Transducer Output When Tank is ¾ Full**

| | CELL 1 | | CELL 2 | | CELL 3 | |
|---|---|---|---|---|---|---|
| R.F. | .634 Hz | .633 Hz | .830 Hz | .830 Hz | .840 Hz | .840 Hz |
| S.D. | .850 in. | 1.250 in. | .034 in. | .067 in. | .129 in. | .222 in. |
| GAGE | μ - in. | μ - in. | μ - in. | μ - in. | μ - in. | μ - in. |
| 36 | 0 | 0 | 0 | 0 | 0 | 0 |
| 37 | 0 | 0 | 0 | 0 | 0 | 0 |
| 38 | 90 | 185 | 0 | 0 | 0 | 90 |
| 39 | * | * | * | * | * | * |
| 40 | * | * | * | * | * | * |
| 41 | 0 | 0 | 0 | 0 | 0 | 0 |
| 42 | 0 | 0 | 0 | 0 | 0 | 0 |
| 43 | 0 | 0 | 0 | 0 | 0 | 0 |
| 44 | 0 | 0 | 0 | 0 | 0 | 0 |
| 45 | 0 | 0 | 0 | 0 | 0 | 0 |
| 46 | * | * | * | * | * | * |
| 47 | * | * | * | * | * | * |
| 48 | 0 | 0 | 0 | 0 | 0 | 0 |
| 49 | 0 | 0 | 0 | 0 | 0 | 0 |
| 50 | * | * | * | * | * | * |
| 51 | 0 | 0 | 0 | 0 | 0 | 0 |
| 52 | * | * | * | * | * | * |
| 53 | 285 | 400 | 0 | 115 | 0 | 230 |
| 54 | 0 | 0 | 0 | 0 | 0 | 0 |
| 55 | 420 | 895 | 130 | 210 | 265 | 395 |
| 56 | 0 | 0 | 0 | 0 | 0 | 0 |
| 57 | 715 | 1140 | 230 | 230 | 170 | 400 |
| 58 | 0 | 0 | 0 | 0 | 0 | 0 |
| 59 | * | * | * | * | * | * |
| 60 | * | * | * | * | * | * |
| 61 | 0 | 0 | 0 | 0 | 0 | 0 |
| 62 | * | * | * | * | * | * |
| 67 | 0 | 0 | 0 | 0 | 0 | 0 |
| 68 | 0 | 0 | 0 | 0 | 0 | 0 |
| 69 | 0 | 0 | 0 | 0 | 0 | 0 |
| 70 | 0 | 0 | 0 | 0 | 0 | 0 |
| 71 | 0 | 0 | 0 | 0 | 0 | 0 |
| 72 | 0 | 0 | 0 | 0 | 0 | 0 |
| 73 | 0 | 0 | 0 | 0 | 0 | 0 |
| 74 | 0 | 0 | 0 | 0 | 0 | 0 |

SYMBOLS: R.F. = Resonant Frequency
S.D. = Shaker Displacement
μ = Micro
* = Bad Gage

Table II. (Concluded)

Transducer Output When Tank is ¾ Full

| | CELL 1 | | CELL 2 | | CELL 3 | |
|---|---|---|---|---|---|---|
| R.F. | .634 Hz | .633 Hz | .830 Hz | .830 Hz | .840 Hz | .840 Hz |
| S.D. | .850 in. | 1.250 in. | .034 in. | .067 in. | .129 in. | .222 in. |
| P.T. | psi | psi | psi | psi | psi | psi |
| 81 | * | * | * | * | * | * |
| 82 | .35 | .50 | .30 | .40 | .60 | .90 |
| 83 | .10 | .15 | .06 | .04 | .04 | .07 |
| 84 | * | * | * | * | * | * |
| 85 | 1.85 | 5.40 | 0 | .55 | .85 | 2.55 |
| 86 | 0 | 0 | 0 | 0 | 0 | 0 |
| 87 | * | * | * | * | * | * |
| 88 | * | * | * | * | * | * |
| 89 | .40 | .60 | .20 | .15 | .10 | .35 |
| 90 | * | * | * | * | * | * |
| 91 | .40 | .65 | 0 | 0 | .08 | .10 |
| 96 | 0 | 0 | 0 | 0 | 0 | 0 |
| 99 | 0 | 0 | 0 | 0 | 0 | 0 |
| 100 | * | * | * | * | * | * |
| 104 | 0 | 0 | 0 | 0 | 0 | 0 |
| 105 | .20 | .30 | 0 | 0 | 0 | 0 |
| 106 | 0 | 0 | 0 | 0 | 0 | 0 |

| S.S.† | Oscillograph Movement and Corresponding (Peak-to-Trough Slosh Movement) (Inches) | | | | | |
|---|---|---|---|---|---|---|
| 160 | .18 (9) | .20 (13½) | .05 (N.A.) | .06(N.A.) | .08(N.A.) | .12(N.A.) |
| 162 | .16 (N.A.) | .20 (N.A.) | .10(5 3/4) | .11(6) | .10(N.A.) | .12(N.A.) |
| 164 | .10 (N.A.) | .15 (N.A.) | .25 (N.A.) | .25(N.A.) | .28(9½) | .35(15½) |
| L.F. | Change in Load While Sloshing (Peak Load-Minimum Load) (Pounds) | | | | | |
| 1 | * | * | * | * | * | * |
| 2 | 1250 | 2100-2230 | 260-330 | 330-395 | 330-395 | 850-985 |
| 3 | * | * | * | * | * | * |
| 4 | 895-1160 | 2500-2860 | 355-445 | 355-445 | 455 | 1160-1520 |
| 5 | 1485-1545 | 2380 | 120-180 | 240-300 | 360 | 715-775 |
| 6 | * | * | * | * | * | * |
| 7 | 1310-1690 | 2250-2500 | 310-435 | 375-560 | 435 | 1250 |
| 8 | * | * | * | * | * | * |
| 9 | 1450 | 2400 | 350 | 350 | 250-450 | 1100 |
| 10 | 800 | 800 | 150 | 200-250 | 250-300 | 650 |
| L.C. | 1000 | 1680 | 200-260 | 220-280 | 180-260 | 840 |

SYMBOLS: R.F. = Resonant Frequency S.S. = Slosh Sensor
S.D. = Shaker Displacement L.F. = Load Feet
P.T. = Pressure Transducer L.C. = Load Cell
N.A. = Not Available * = Bad Gage

†NOTE: The actual slosh movement is not linearly proportional to oscillograph movement.

Observation of Figure 10 for force in x direction for the 1/2-full case shows the test points to be much below the theoretical curve. This discrepancy can be attributed to several factors. First, the test values were obtained at forcing frequencies very near the natural frequencies of the liquid. When this occurs, nonlinearities of the liquid behavior in each of the cells cause poor correlations to linearized theory. This has been observed in other tests (Reference 3). Second, the theoretical curve is based on undamped linear motion of the liquid. In the actual test tank, however, the stiffeners and other structure in the cells have a damping effect on the liquid. If damping terms were added to the theoretical expressions, it is believed that better correlations would have occurred. Third, the method of force measurement by gage on the shaker arm may have caused the force readings to be low due to a phase lag of liquid sloshing and shaker arm displacement.

Observation of Figure 11 for force in the x direction for the 3/4-full case shows somewhat better agreement between measured and theoretical values, especially at points near the second natural frequency. For the 3/4-full test, a smaller percentage of the total liquid mass is sloshing, which may account for better correlation of force data.

It would have been desirable to have measured force at frequencies other than those so close to the natural frequency. It is believed that better correlation would have been obtained.

## C. Moments

The theoretical expressions for moment in Section IV-E are about the x' and y' axes (Figure 7) or about the center of the liquid. The experimental values of moment will have to be determined by the ten load feet readings at the bottom of the tank for each test case. Therefore, a total theoretical moment on the load feet was determined by consideration of the combined effect of the moment at the center of the tank plus the moment caused by the lateral sloshing forces. Thus, curves were plotted for total moment on the load feet, about both the x and y axes for both 1/2- and 3/4-full test condition, versus the forcing frequency ( $\Omega$ ). These plots are shown in Figures 14, 15, 16, and 17, with the two vertical broken lines representing the first two liquid natural frequencies.

The ten load feet readings for the 1/2- and 3/4-full test conditions are given in Tables I and II. Several difficulties were encountered in converting these readings to moment values about the x and y axes which made correlation extremely difficult. First, the readings were not time-correlated as given. Second, there were several load feet gages that were bad, especially in the 3/4-full test. This required the assumption of values at these feet to determine moments. Third, several load feet readings varied considerably during the test, making it necessary to average load readings.

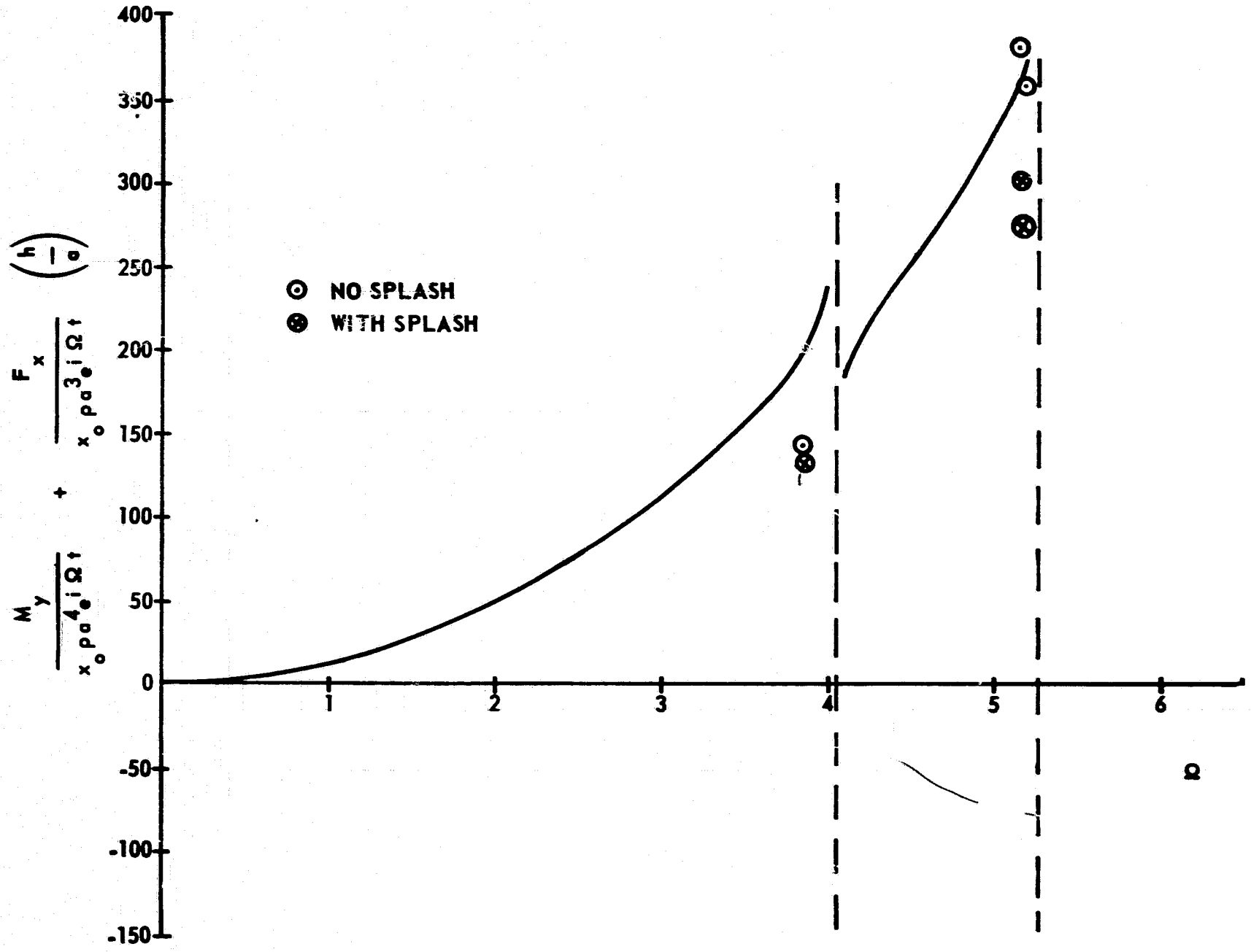


FIGURE 14. TOTAL MOMENTON LOAD FEET ABOUT Y AXIS FOR 1/2-FULL TANK VERSUS FORCING FREQUENCY

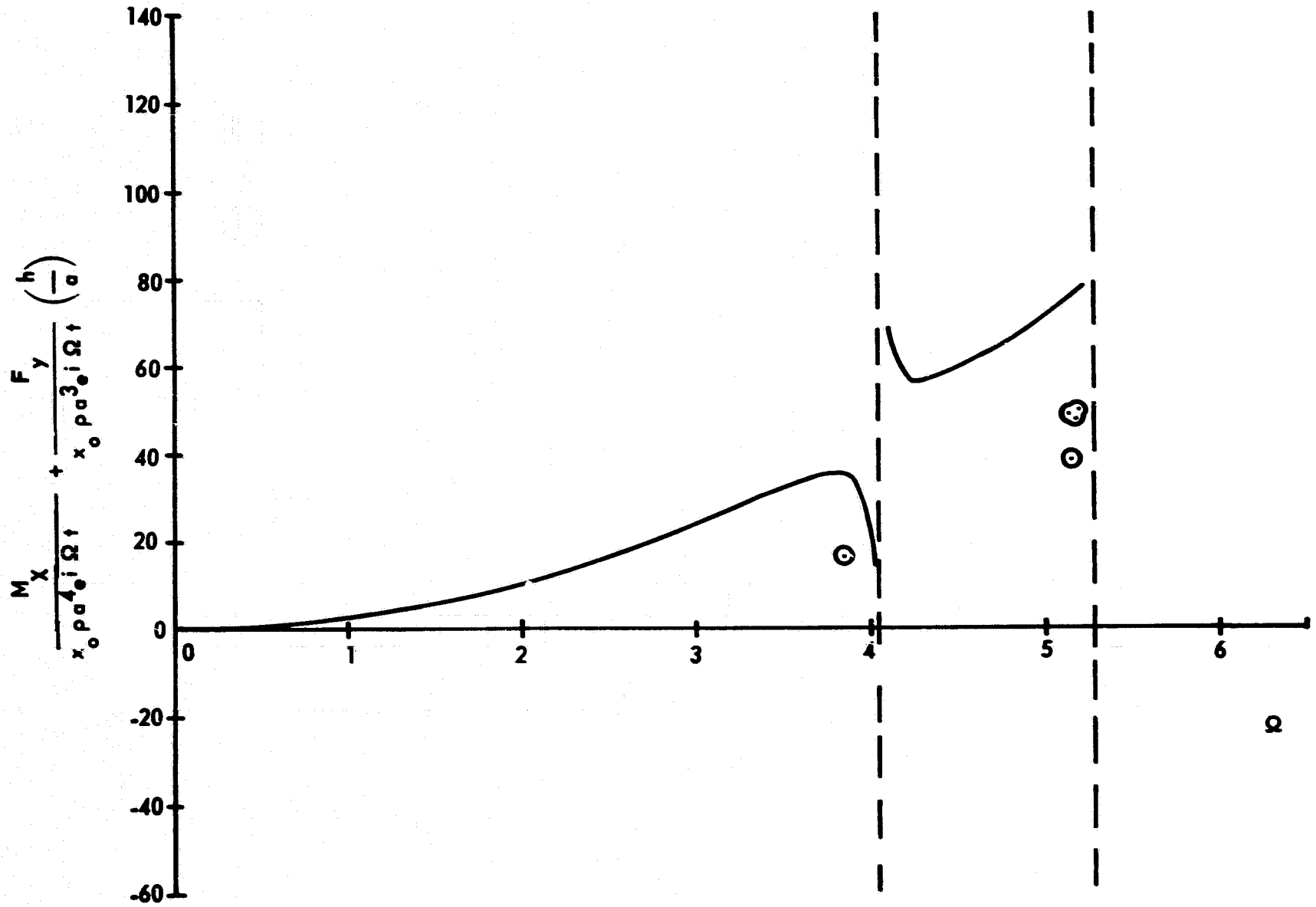


FIGURE 15. TOTAL MOMENT ON LOAD FEET ABOUT X AXIS FOR 1/2- FULL TANK VERSUS FORCING FREQUENCY

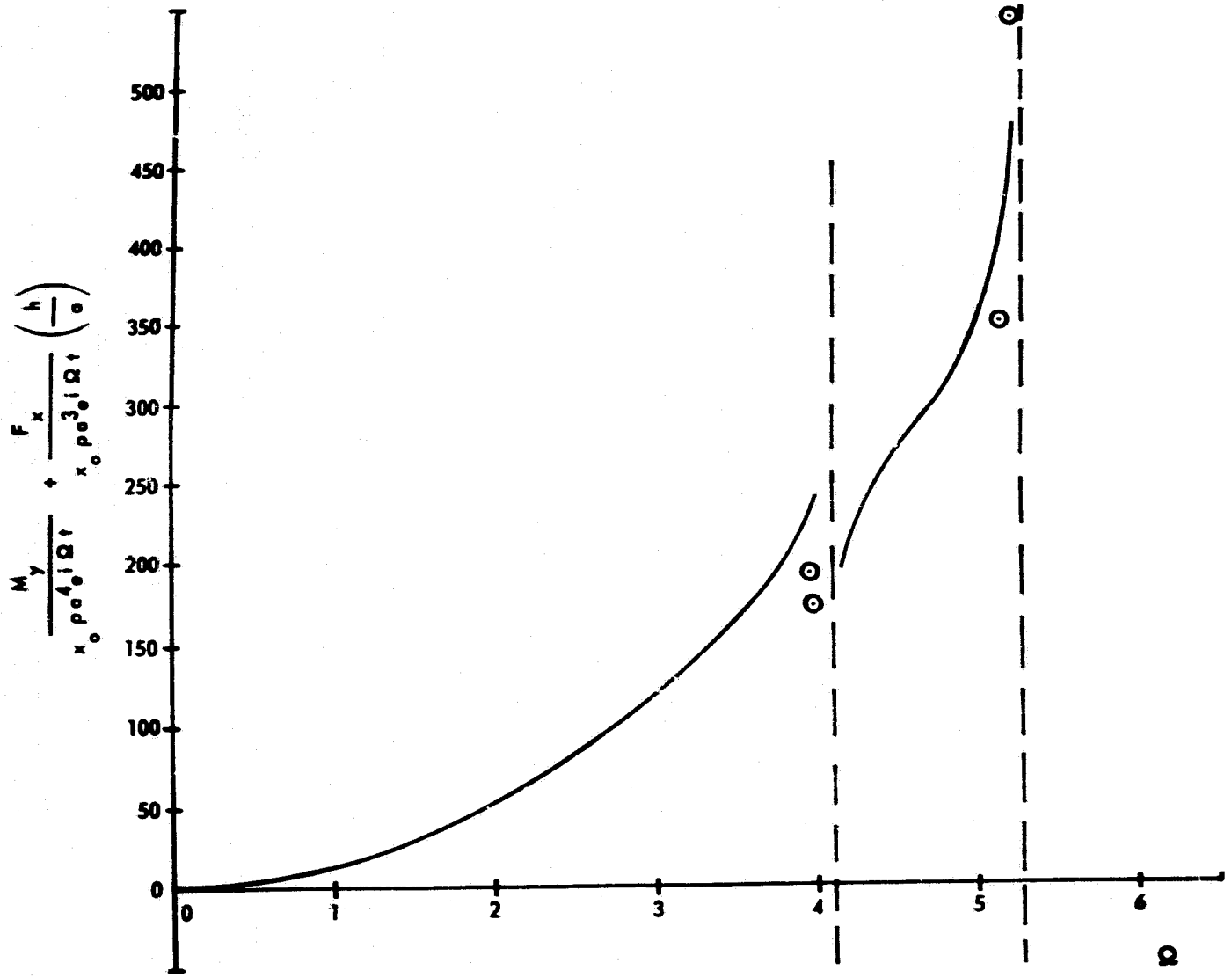


FIGURE 16. TOTAL MOMENT ON LOAD FEET ABOUT Y AXIS FOR 3/4-FULL TANK VERSUS FORCING FREQUENCY

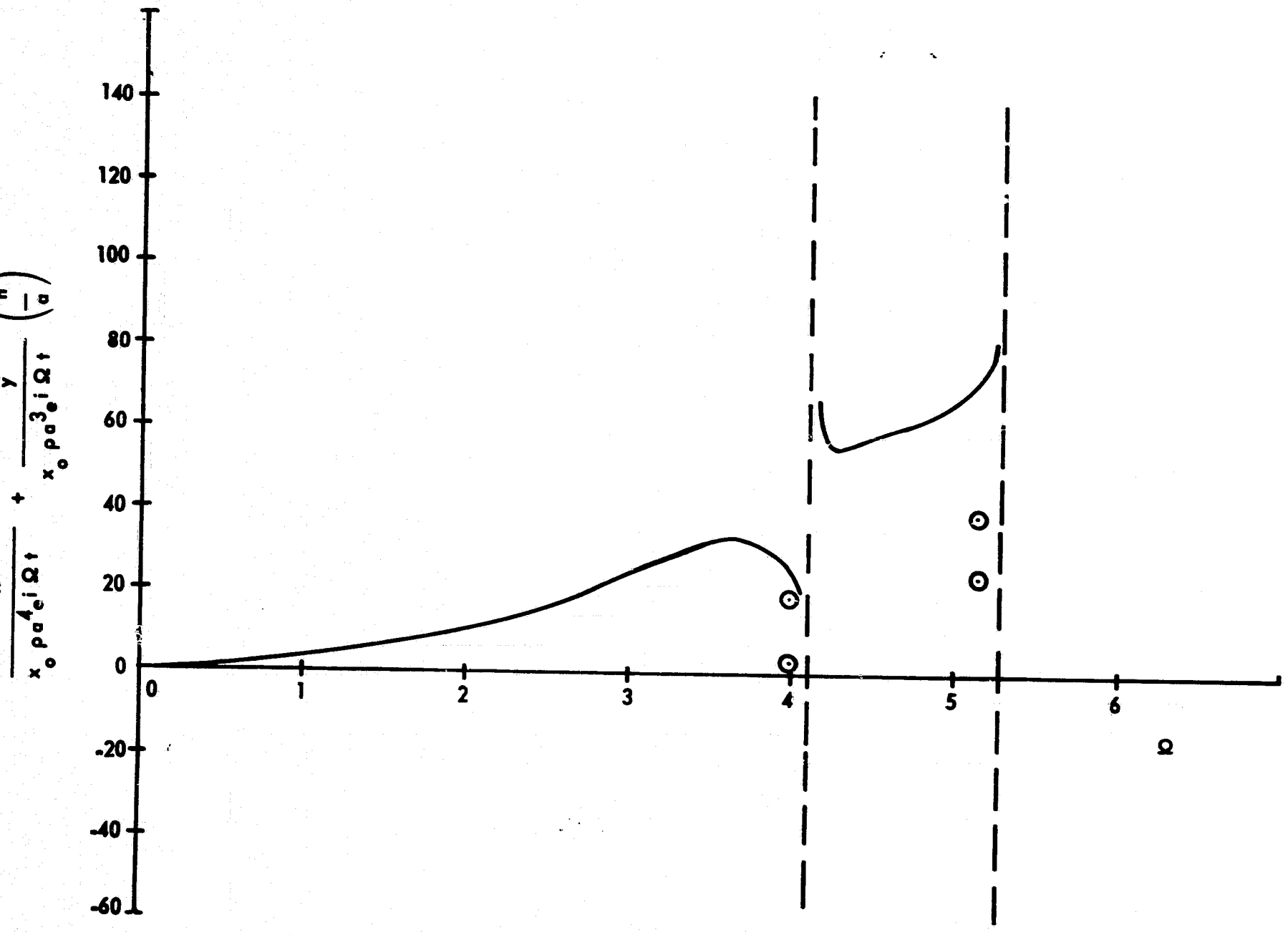


FIGURE 17. TOTAL MOMENT ON LOAD FEET ABOUT X AXIS FOR 3/4-FULL TANK VERSUS FORCING FREQUENCY

1. 1/2-Full Condition

The values of moment on the load feet calculated from the load feet readings are plotted in Figures 14 and 15 for the 1/2-full condition. The test results for moment about the y axis agree very well with the theoretical curve, especially with the results obtained when cells 2 and 3 are sloshing at their natural frequencies.

The plotted results for moment about the x axis do not agree as well as results for moment about the y axis. However, since the moment about the x axis is much smaller in magnitude than the moment about the y axis, slight variations in load cell readings will greatly affect the moment calculation. Also, the assumptions and the averaging techniques used to determine the moments had some effect on the accuracy.

2. 3/4-Full Condition

Results for the 3/4-full condition are plotted in Figures 16 and 17. When cell 2 is in resonance the results appear to be bad; shaker displacement readings for this condition appear to be faulty. The values obtained are not greatly at variance with expected results considering that four of the ten load feet were not reading properly.

The results for moment about the x axis are low due to the same reasons discussed above.

## D. Surface Displacements

The theoretical expression for surface displacement in a single cell (given in Section IV-F) was used for this evaluation. This expression was evaluated for each cell at the outer radius of the cell (r = a) for excitation amplitude and forcing frequency equal to the maximum nonsplash frequency for cells 1, 2, and 3 at the 1/2-full condition. These results are given in Figures 18, 19, and 20. These figures show the shape and displacement of the surface in each of the three cells for the conditions given. The radial mode of cell 1 and the tangential modes of cells 2 and 3 can be seen.

The surface shapes for these conditions observed by the television cameras were very close to those shown in Figures 18, 19, and 20. However, the observed surface displacements were much greater than those calculated. This can be explained by the fact that linear theory was used to predict the surface displacement; whereas, the actual displacement, close to the natural frequency of the liquid, is nonlinear.

## E. Pressure

The pressure at any point in any point in any cell can be evaluated by the expression given in Section IV-C.

The pressure transducer output for the transducer locations shown

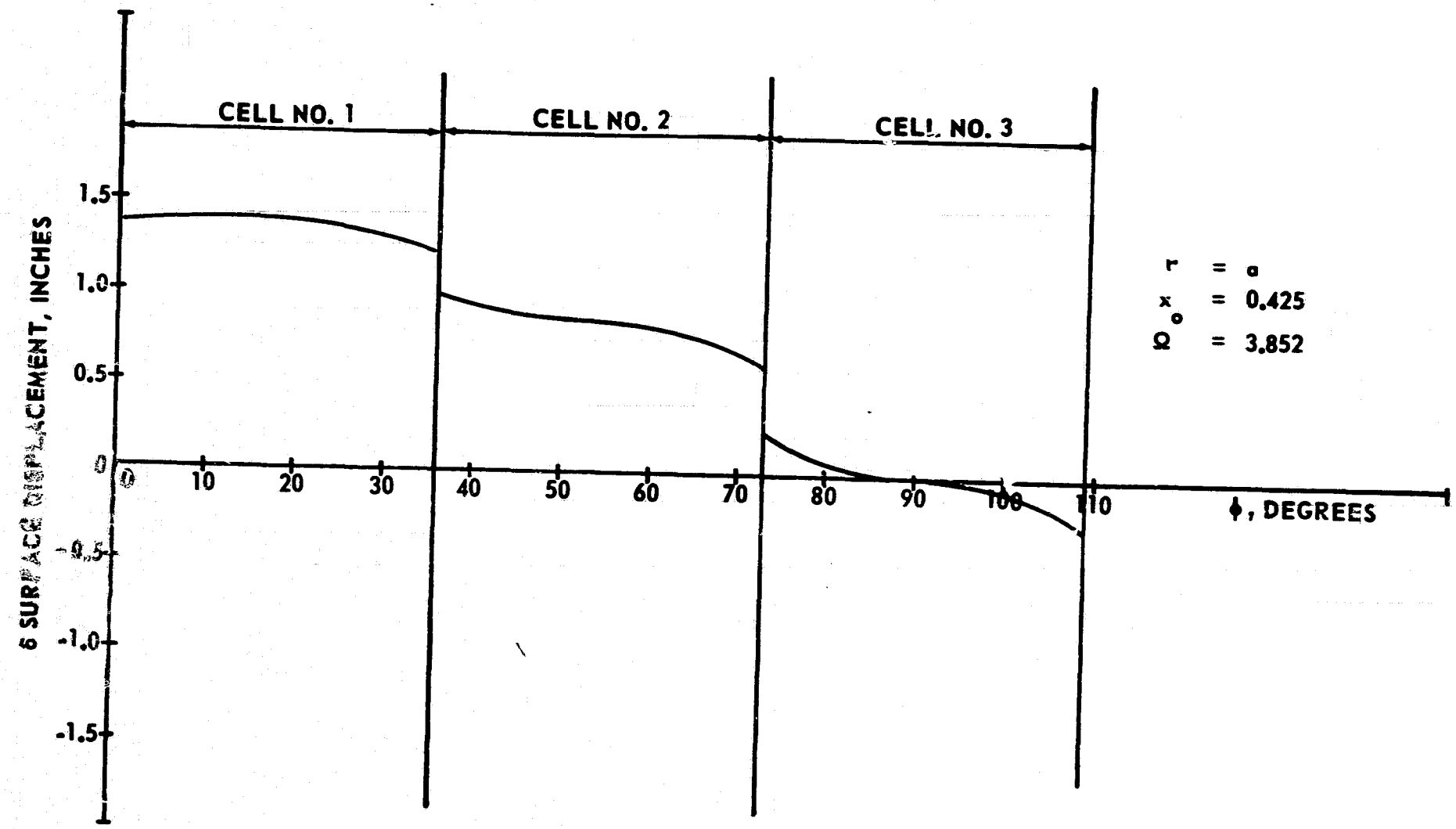


FIGURE 18. SURFACE DISPLACEMENTS, CELL 1 IN RESONANCE, 1/2-FULL TANK

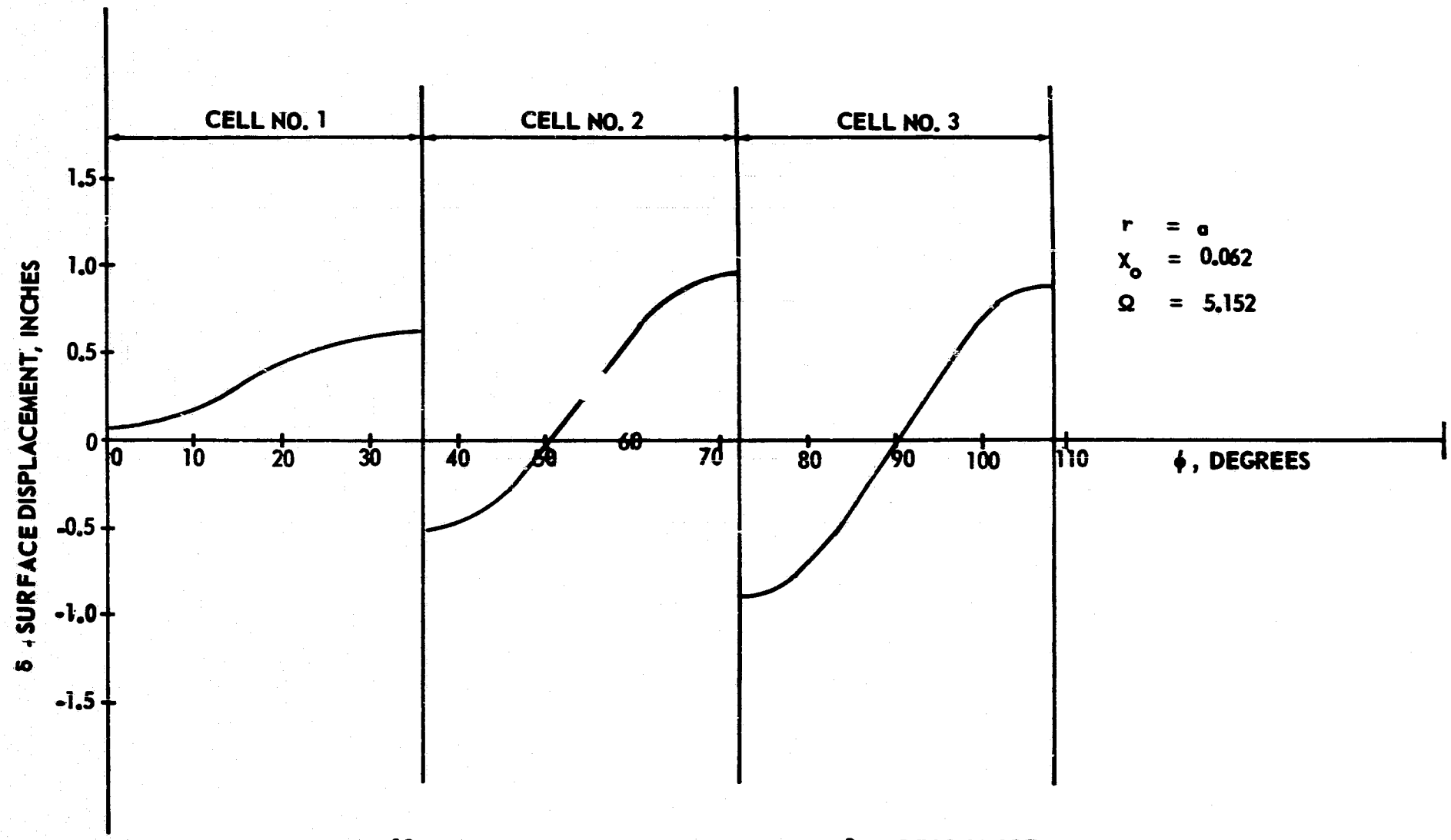


FIGURE 19. SURFACE DISPLACEMENTS, CELL 2 IN RESONANCE, 1/2-FULL TANK

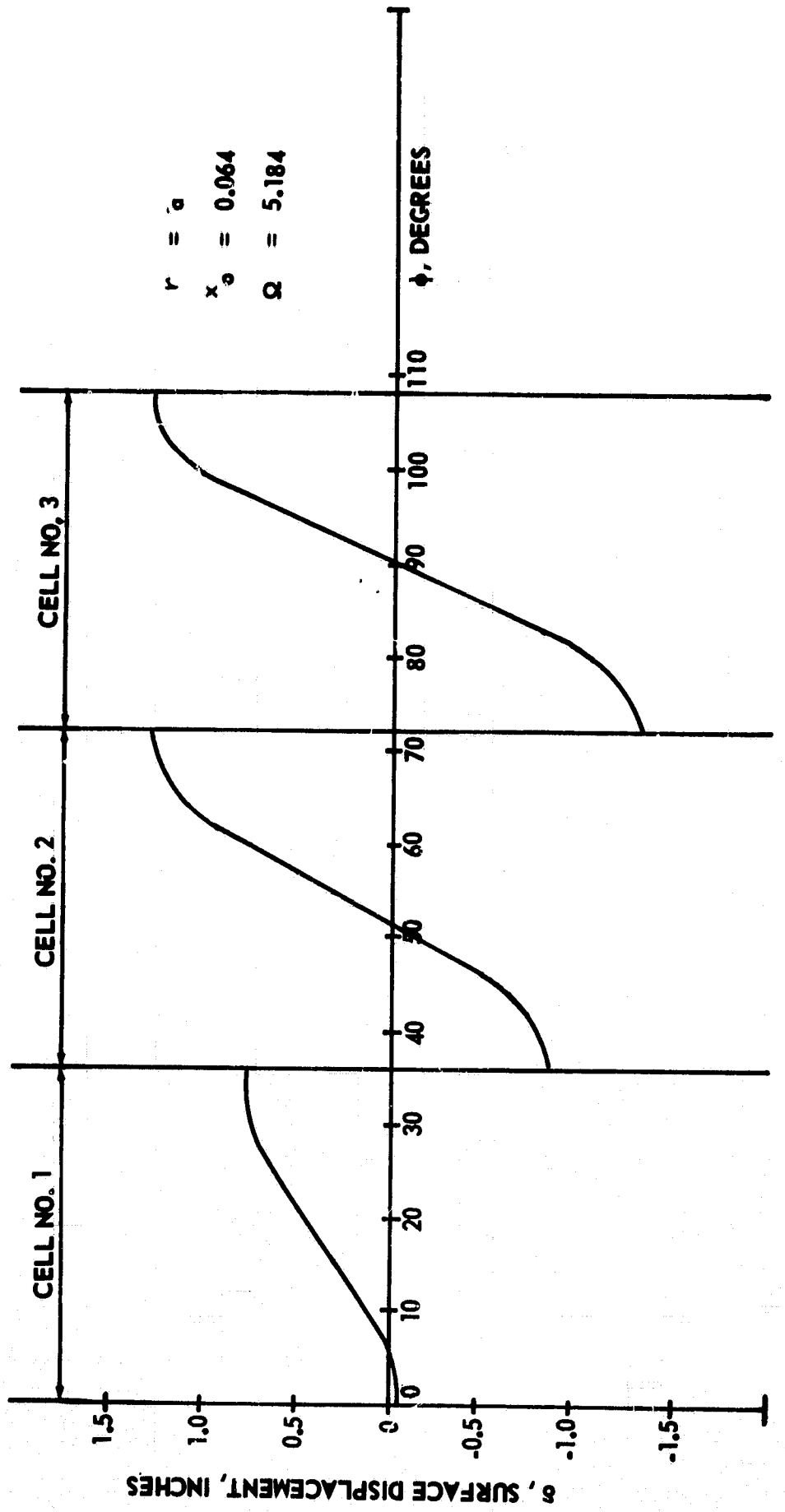


FIGURE 20. SURFACE DISPLACEMENTS, CELL 3 IN RESONANCE, 1/2-FULL TANK

in Figure 2 is given in Tables I and II. The readings given are due only to pressure differentials caused by the sloshing liquid, as static liquid pressure has been subtracted. Approximately one-third of the pressure transducers gave bad readings, and several other transducers gave no reading at all; therefore, data was limited.

Pressures were calculated, from the theoretical expression, for transducers that appeared to give good readings. The calculated values of pressure due to the sloshing liquid were much smaller than the pressures obtained from the transducers. Again, this can be explained by the fact that linear theory was used and nonlinear sloshing was occurring. The pressure reading is directly related to the surface amplitudes obtained in Section D.

## F. Strain Gage Readings

Strain gages, located as shown in Figure 2, gave readings as presented in Tables I and II. From the data it is seen that about two-thirds of the gages were bad or gave zero strain readings. All the strain readings that were obtained were of relatively low magnitude. Actually, this situation is to be expected, considering the low amplitudes of the sloshing liquid in the individual cells. The only strain that occurs is due to the differential of pressure across a cell wall due to wave height differentials like those shown in Figure 20. The small strain readings also indicate that the structural configuration of the multicell is quite rigid. As long as the liquid is sloshing at low amplitudes, there appears to be no possibility of overstressing the cell walls.

## SECTION VI. CONCLUSIONS AND RECOMMENDATIONS

Based on the correlation and evaluation of theoretical analysis and experimental data the following conclusions and recommendations are indicated.

For a circular cylindrical tank with no cell walls and with the same geometry and liquid height corresponding to the 1/2-full condition as shown in Figure 7, the first natural frequency is 0.303 hertz and approximately 40 percent of the liquid is sloshing (Ref. 4). For the tenth-sectored tank the first natural frequency is 0.643 hertz and approximately 10 percent of the liquid is sloshing. Therefore, the advantages of the compartmented tank in raising the first natural frequency and in reducing the percentage of sloshing liquid mass are confirmed.

The equivalent circular cylindrical sectored tank used for the theoretical analysis was quite adequate to predict the sloshing behavior of the liquid in the Multicell Tank.

The natural frequencies of the liquid obtained by test were very close (within 5 percent) to those obtained from theory, as applied to the equivalent tank.

The data obtained for the force in the x direction and for moments on the load feet were in good agreement with theory, considering that the results were obtained at frequencies near resonance where liquid behavior is erratic, and considering the limited gage readings on the load feet.

Surface sloshing amplitudes were not large enough to give significant readings on the pressure transducers and strain gages located within the tank.

It was apparent that additional instrumentation would have been useful; for example, the yoke on which the guide roller wheel was mounted could have been equipped with strain gages to measure the induced lateral force in the y direction. Additionally, an accelerometer mounted on the specimen parallel to (and in close proximity to) the shaker axis would have provided additional force information for comparison with the theoretical results.

# APPENDIX A

## Sectored Tank Theoretical Expressions

## APPENDIX A. Sector Tank

Container: The container (Refer to Figure 6) is a sector of a right circular cylinder of radius a; it is filled with a liquid to a depth h. The vertex angle is denoted by $\bar{\alpha}$

Coordinate System: The origin is located at the center of gravity of the undisturbed fluid which would be contained in a right circular cylinder generated by revolving the sector tank about the z axis. The x axis must lie in the sector wall.

Comments: The results given in this section are not valid for

$\bar{\alpha} = \pi/2 , \ 3\pi/2$

Translation in the x direction, $x = x_o e^{i\Omega t}$ and translation in the y direction, $y = y_o e^{i\Omega t}$

1. Boundary Conditions:

(a) $$\left(\frac{\partial \Phi}{\partial r}\right)_{r=a} = i\Omega \left\{ \begin{matrix} x_o \\ y_o \end{matrix} \right\} e^{i\Omega t} \left\{ \begin{matrix} \cos\phi \\ \sin\phi \end{matrix} \right\}$$

(b) $$\left(\frac{\partial \Phi}{\partial z}\right)_{z=-h} = 0$$

(c) $$\left(\frac{1}{r}\frac{\partial \Phi}{\partial \phi}\right)_{\phi=0} = \left\{ \begin{matrix} 0 \\ i\Omega y_o e^{i\Omega t} \end{matrix} \right\}$$

(d) $$\left(\frac{1}{r}\frac{\partial \Phi}{\partial \phi}\right)_{\phi=\bar{\alpha}} = -i\Omega \left\{ \begin{matrix} -x_o \\ y_o \end{matrix} \right\} e^{i\Omega t} \left\{ \begin{matrix} \sin\bar{\alpha} \\ \cos\bar{\alpha} \end{matrix} \right\}$$

(e) $$\left(\frac{\partial^2 \Phi}{\partial t^2} + g\frac{\partial \Phi}{\partial z}\right)_{z=0} = 0$$

2. Velocity Potential:

$$\Phi = \begin{Bmatrix} \bar{i}\Omega\, x_o \\ \bar{i}\Omega\, y_o \end{Bmatrix} e^{i\Omega t} \left[ \begin{Bmatrix} r\cos\phi \\ r\sin\phi \end{Bmatrix} + \frac{b_{mn}\,\eta^2}{(1-\eta^2)} \begin{Bmatrix} a_m \\ c_m \end{Bmatrix} \cos(\phi)\ \frac{\cosh(\kappa+\zeta)}{\cosh\kappa}\ J(\sigma) \right].$$

3. Natural Angular Frequency:

$$\omega_{mn}^2 = \frac{g}{a}\,\epsilon_{mn}\tanh\kappa \quad , \text{ where } \epsilon_{mn} \text{ are roots of } J'_{m/2\alpha}(\epsilon_{mn}) = 0 .$$

4. Forces and Moments:

$$F_x = M_f\,\Omega^2 e^{i\Omega t} \begin{Bmatrix} x_o \\ y_o \end{Bmatrix} \left[ \begin{Bmatrix} 1 \\ 0 \end{Bmatrix} + \frac{2\sin\bar{\alpha}\, b_{mn}\,\eta^2}{\bar{\alpha}a\,(1-\eta^2)} \begin{Bmatrix} a_m \\ c_m \end{Bmatrix} (-1)^{m+1}\ \frac{\tanh\kappa}{\kappa} \left\{ \frac{\bar{\alpha}^2}{(\pi^2 m^2 - \bar{\alpha}^2)} J(\epsilon_{mn}) + L_o(\epsilon_{mn}) \right\} \right].$$

$$F_y = M_f\,\Omega^2 e^{i\Omega t} \begin{Bmatrix} x_o \\ y_o \end{Bmatrix} \left[ \begin{Bmatrix} 0 \\ 1 \end{Bmatrix} - \frac{2\,b_{mn}\,\eta^2}{\bar{\alpha}\,a\,(1-\eta^2)} \begin{Bmatrix} a_m \\ c_m \end{Bmatrix} \left[ 1 - (-1)^m \cos\bar{\alpha} \right] \frac{\tanh\kappa}{\kappa} \left\{ \frac{\bar{\alpha}^2}{(\pi^2 m^2 - \bar{\alpha}^2)} J(\epsilon_{mn}) + L_o(\epsilon_{mn}) \right\} \right].$$

$$M_x = -M_f \Omega^2 e^{i\Omega t} a \begin{Bmatrix} x_o \\ y_o \end{Bmatrix} \left[ \begin{Bmatrix} \frac{1}{4\frac{h}{a}} \frac{2\sin^2\bar{\alpha}}{\bar{\alpha}} \\ \frac{1}{4\frac{h}{a}} \quad 1 - \frac{\sin\bar{\alpha}\cos\bar{\alpha}}{\bar{\alpha}} \end{Bmatrix} - \right.$$

$$\frac{1}{\bar{\alpha} a} \frac{b_{mn}\eta^2}{(1-\eta^2)} \begin{Bmatrix} a_m \\ c_m \end{Bmatrix} \frac{1}{\epsilon_{mn}} \left[ 1 - (-1)^m \cos\bar{\alpha} \right] \left\{ \left[ \frac{\bar{\alpha}^2}{(m^2\pi^2 - \bar{\alpha}^2)} J(\epsilon_{mn}) + L_o(\epsilon_{mn}) \right] \right.$$

$$\left. \left[ \tanh\kappa + \frac{2}{\kappa}\left(\frac{1}{\cosh\kappa} - 1\right) \right] + \frac{2\bar{\alpha}^2 \epsilon_{mn}^2 L_2(\epsilon_{mn})}{(m^2\pi^2 - \bar{\alpha}^2)\kappa\cosh\kappa} \right\} \left. \right] - 2M_f g \frac{a}{3} \frac{(1-\cos\bar{\alpha})}{\bar{\alpha}} .$$

$$M_y = M_f \Omega^2 e^{i\Omega t} a \begin{Bmatrix} x_o \\ y_o \end{Bmatrix} \left[ \begin{Bmatrix} \frac{4}{\frac{h}{a}} \left(1 + \frac{\sin\bar{\alpha}\cos\bar{\alpha}}{\bar{\alpha}}\right) \\ \frac{4}{\frac{h}{a}} \frac{\sin^2\bar{\alpha}}{\bar{\alpha}} \end{Bmatrix} + \right.$$

$$\frac{\sin\bar{\alpha}\,(-1)^{m+1}}{a\bar{\alpha}\,\epsilon_{mn}} \frac{b_{mn}\eta^2}{(1-\eta^2)} \begin{Bmatrix} a_m \\ c_m \end{Bmatrix} \left\{ \left[ \frac{\bar{\alpha}^2}{(m^2\pi^2 - \bar{\alpha}^2)} J(\epsilon_{mn}) + L_o(\epsilon_{mn}) \right] \right.$$

$$\left. \left[ \tanh\kappa \quad \frac{2}{\kappa}\left(\frac{1}{\cosh\kappa} - 1\right) \right] + \frac{2\bar{\alpha}^2 \epsilon_{mn} L_2(\epsilon_{mn})}{(m^2\pi^2 - \bar{\alpha}^2)\,\kappa\cosh\kappa} \right\} \left. \right] + 2M_f g \frac{a}{3} \frac{\sin\bar{\alpha}}{\bar{\alpha}} .$$

5. Constants:

$$a_o = \frac{\sin\bar{\alpha}}{\bar{\alpha}} \quad , \quad a_m = \frac{2\bar{\alpha}\,(-1)^{m+1}\sin\bar{\alpha}}{(m^2\pi^2 - \bar{\alpha}^2)} \quad , \quad m = 1, 2, 3 \ldots$$

$$b_{mn} = 2a\,\frac{\dfrac{\Gamma\left(\frac{m}{4\alpha} + \frac{3}{2}\right)}{\Gamma\left(\frac{m}{4\alpha} - \frac{1}{2}\right)} \sum_{\mu=0}^{\infty} \frac{\left(\frac{m}{2\alpha} + 2\mu + 1\right)\,\Gamma\left(\frac{m}{4\alpha} + \mu - \frac{1}{2}\right)}{\Gamma\left(\frac{m}{4\alpha} + \mu + \frac{5}{2}\right)} J_{(m/2\alpha)+2\mu+1}(\epsilon_{mn})}{\epsilon_{mn}\left(1 - \frac{m^2}{4\alpha^2\epsilon_{mn}^2}\right) J_{m/2\alpha}(\epsilon_{mn})} \qquad m, n = 0, 1, 2 \ldots$$

$$c_o = \frac{1 - \cos\bar{\alpha}}{\bar{\alpha}} \quad , \qquad c_m = \frac{2\bar{\alpha}\left[(-1)^m \cos\bar{\alpha} - 1\right]}{(m^2\pi^2 - \bar{\alpha}^2)} \quad , \quad m = 1, 2, 3 \ldots$$

$$L_2(\epsilon_{mn}) = \frac{\Gamma\left(\frac{m}{2\alpha} + \frac{3}{2}\right)}{\epsilon_{mn}\,\Gamma\left(\frac{m}{2\alpha} - \frac{1}{2}\right)} \sum_{\mu=0}^{\infty} \frac{\left(\frac{m}{2\alpha} + 2\mu + 1\right)\,\Gamma\left(\frac{m}{4\alpha} + \mu - \frac{1}{2}\right)}{\Gamma\left(\frac{m}{4\alpha} + \mu + \frac{5}{2}\right)} J_{(m/2\alpha)+2\mu+1}(\epsilon_{mn})$$

$$L_o(\epsilon_{mn}) = \frac{2}{\epsilon_{mn}} \sum_{\mu=0}^{\infty} J_{2\mu+(m/2\alpha)+1}(\epsilon_{mn}) \qquad \eta = \frac{\Omega}{\omega_{mn}} \quad , \quad \zeta = \epsilon_{mn}\frac{z}{a}$$

$$\sigma = \epsilon_{mn}\frac{r}{a} \quad , \qquad \kappa = \epsilon_{mn}\frac{h}{a} \qquad \bar{\alpha} = 2\pi\alpha \quad , \quad M_f = \rho\pi a^2 h\alpha$$

# APPENDIX B

## Constants for Tenth-Sector Tank

## APPENDIX B

### CONSTANTS FOR TENTH SECTOR TANK ( $a = 1/10$)
(References 6 & 7)

1. Roots of $J'_{5m}(\xi_{mn}) = 0$ $(\epsilon_{mn})$

| n \ m | 0 | 1 | 2 |
|---|---|---|---|
| 0 | 3.832 | 6.416 | 11.716 |
| 1 | 7.016 | 10.520 | 16.448 |
| 2 | 10.173 | 13.987 | 20.223 |
| 3 | 13.324 | 17.313 | 23.761 |
| 4 | 16.471 | 20.576 | 27.182 |

2. $a_o$, $a_m$

| m | $a_m$ |
|---|---|
| 0 | .93551 |
| 1 | .07795 |
| 2 | -.01889 |
| 3 | .00835 |
| 4 | -.00468 |

3. $b_{mn}$

| n \ m | 0 | 1 |
|---|---|---|
| 0 | -.57778a | 2.909a |
| 1 | .0747a | .7395a |
| 2 | -.10504a | |

4. $C_m$

| m | $C_m$ |
|---|---|
| 0 | .30398 |
| 1 | -.23992 |
| 2 | -.00614 |
| 3 | -.02570 |
| 4 | -.00152 |

5. $L_o$ ( $\epsilon_{mn}$)

| n \ m | 0 | 1 |
|---|---|---|
| 0 | .28498 | .12059 |
| 1 | .13675 | .09931 |
| 2 | .10066 | - |

6. $L_2(\epsilon_{mn})$

| n \ m | 0 | 1 |
|---|---|---|
| 0 | -.04686 | .07938 |
| 1 | .00336 | .01915 |
| 2 | -.00327 | |

## REFERENCES


1. Cooper, F., "Test Procedures for the 200-Inch Multicell Tank Slosh Test," Brown Engineering, BECO-3450-M-9, November 2, 1967.

2. Cooper, F., "200-Inch Multicell Tank Slosh Tests," Brown Engineering, CR-61244, November 29, 1968.

3. Abramson, H. N., "The Dynamic Behavior of Liquids in Moving Containers," NASA SP-106, 1966.

4. Bauer, H. F., "Fluid Oscillations in the Containers of a Space Vehicle and Their Influence upon Stability," NASA TR R-187, February, 1964.

5. Kirkman, D., "Graphs and Formulas of Zeros of Cross Product Bessel Functions," Journal of Mathematics and Physics, (1958).

6. Jahnke, E. and Emde, F., "Tables of Functions with Formulae and Curves," Dover Publications, N. Y., 1945.

7. Staff, Harvard University Computation Laboratory: "Tables of the Bessel Functions." Harvard University Press, Cambridge, Mass., 1946.